T H E U N I V E R S I T Y O F M I C H I G A N
COLLEGE OF ENGINEERING
Department of Mechanical Engineering

Student Project Reports

INVESTIGATION OF DESIGN MEANS FOR HOME LAUNDRY APPLIANCES

James G. Morgan
Gee-In-Goo
Vern Wedeven
Douglas H. Lane

ORA Project 07494

under contract with:

Whirlpool Corporation
Benton Harbor, Michigan

administered through:

OFFICE OF RESEARCH ADMINISTRATION ANN ARBOR

June 1966

TABLE OF CONTENTS

TABLE OF CONTENTS (Continued)

INVESTIGATION OF MEANS OF DESIGNING PUMPS HAVING THE OUTPUT CHARACTERISTICS AND POWER DEMAND USED IN HOME LAUNDRY APPLIANCES

James G. Morgan

ABSTRACT

This report is an investigation of means of designing pumps having the output characteristics and power demands used in home laundry appliances. These are essentially low-flow-rate, low-head pumps.

Four areas have been investigated:

(1) Analytical Analysis
(2) Computer Program
(3) Design
(4) Testing

Discussion of the first three areas is included in this report. The area of testing is to be studied further during the Fall semester. The most promising design procedures for volute and impeller are outlined in detail. Other possible methods are mentioned and considered briefly. A final report will be submitted in December, 1966.

INTRODUCTION

A program was initiated in September, 1965, at The University of Michigan to formulate a procedure for using modern computer techniques in designing centrifugal pumps. The two basic requirements of the procedure are that it require persons unskilled in pump design to specify only a small number of operating parameters, and that with this information, the program spell out completely the pump geometry that will produce the necessary operating conditions.

This investigation is essential, because current procedures of designing centrifugal pumps are often expensive, inaccurate, and unpredictable. Information regarding pump operation, installation, maintenance, selection, etc., is quite plentiful. However, due to extreme competition between pump manufacturers, little usable knowledge regarding analytical design has been made available to the engineering profession. Furthermore, the few analytical-empirical techniques available through professional organization literature and texts are intended essentially for operation at large heads (30-100 ft.) and extremely high-flow rates (200-2000 gpm) relative to the range of operation normally encountered in general appliance application (approx. 10 ft and 10 gpm).

Moreover, most of the literature about pump design deals essentially with clear water pumping media. However, this is definitely not the case encountered in washing machines. The pumps employed in washing machines are unique in that they must be able to effectively pump water that may be contaminated with large quantities of dirt, soap suds, long strings of clothes lint, and, upon occasion, even a ball point pen.

This project would represent an important technological advancement; as far as I know no satisfactory computerized pump design is generally available in industry. Basically, the computer program will require the designer to supply the desired operational data (i.e., flow rate, head, shaft speed, etc.) to the computer. The computer output, when applied, will specify all the geometrical parameters (i.e., impeller diameter, vane height, inlet and outlet blade angles, housing dimensions, minimum shaft size, etc.) and the additional information required to manufacture a pump that will operate under specified conditions.

With a program of this nature, an occasional pump designer or technician can determine relatively simple pump requirements and in a few minutes have "ball park" answers to satisfactorily fabricate a pump that would operate at the specified operating conditions. Indeed, the implications suggested here are tremendous.

The use of this technique would result in substantial cost and time savings in engineering, drafting, and model work. In addition, it would save the time and money normally expended for review when personnel involved design pumps infrequently.

The report format has been divided into the following areas to facilitate discussion:

(1) An analytical analysis to formulate pump variables in terms of mathematical expressions.

(2) A computer program based on these mathematical expressions.

(3) Design for a small number of prototypes based on research and analysis.

(4) Testing program.

Discussion of the first three phases is included in this report. A prototype is being fabricated by Whirlpool in St. Joseph, Michigan, and is expected to be ready for testing near the end of the Spring semester. In addition, a test has been run on the present production pump used in the Whirlpool combination washer and dryer. The results of this test are enclosed.

DISCUSSION

As noted in the introduction, the major problems associated with this investigation are:

(1) Present design methods are expensive and unreliable.

(2) Theoretical fluid mechanics cannot adequately predict pump performance.

(3) Business competition has stymied publication of pump design information.

(4) Little information has been published concerning low-flow-rate, low-head, centrifugal pumps.

(5) The pumping medium is unique.

The pump discussed in this report is a centrifugal pump with the following characteristics: horizontal shaft, single entry along the shaft (eye), tangential outlet, open-faced curved blades with variable height. It will be designed to operate between 10-20 ft of head, 10-20 gpm, and at a number of constant speeds.

ANALYTICAL ANALYSIS

Methods of centrifugal pump design are anything but standardized. Centrifugal pump practice is usually based on the historical one-dimensional flow hypothesis governed by Bernoulli's equation, although it has been shown experimentally to be three-dimensional. Let us take a clear look at the assumptions necessary to obtain this equation from the general energy equation.

$$P/d + h + V^2/2g = \text{constant} \qquad \text{Bernoulli's Equation}$$

Assumptions:

(1) Frictionless fluid
(2) Steady flow
(3) No vorticity
(4) No mechanical loss
(5) Flow along a streamline

Further, the impeller has an infinite number of blades. Thus, a nonturbulent, frictionless fluid flowing through an impeller with an infinite number of blades is assumed. It is readily apparent that the expressions derived from this one-dimensional theory cannot accurately describe normal pump operation where the actual number of blades is small, where friction is a relevant phenomena, and where a very turbulent flow condition with vortices, reversed flow, and eddy currents exists. Recognition of this fact has motivated investigators to introduce a theory based on more orthodox fluid mechanics. Some investigations have employed a three-dimensional approach to describe the flow for incompressible and inviscid flow through mixed-flow turbomachines. Other attempts have been associated with analysis employing the basic assumptions of potential flow. The Japanese have been quite active in this field. Additional highly sophisticated work (boundary layer theory) has been proposed to aid the designer. While literature describing these investigations provides added insight into the physics of the problem, it is seldom of value to the designer because of the complexity of the formulation, the idealized concept of known velocity profiles, and the fact that even with this mathematical sophistication these analyses must assume a frictionless, nonturbulent medium in order to obtain solutions to the differential equations a condition which noted above, is not the true physical case.

Consequently, the standard practice is to use a general, classical, one-dimensional approximation as a guide based on the general laws of centrifugal pump operations, with the realization that the analysis will have to be corrected by factors determined from actual experience and tests.

This report attempts to combine the best of both worlds mentioned above. Mathematical analysis will be employed where it describes the physical case and supplies answers that normally are found through a costly trial and error process. Where little is obtained from increased mathematics and complexity, the answers will be ascertained in another manner. I have employed this approach because I feel that, in combination, a workable procedure can be formulated based on the fundamentals of fluid mechanics plus additional knowledge obtained while undergoing formal engineering training, that will predict satisfactory operating conditions.

A literature search was conducted to investigate possible methods of centrifugal pump design. This research has brought to light the following as possible techniques in formulating a centrifugal pump design procedure:

(1) Impeller and volute design with given loading distribution.
(2) NASA turbine pump design procedure.
(3) Potential flow theory design.
(4) Conventional procedures based on one-dimensional flow and experience.

The first method employs basic fluid mechanics rather than "years-of-experience techniques" as a criteria for centrifugal pump design. According to this method, formulated by Professor A. G. Hansen of the University of Michigan, the blade loading is described analytically in a polar coordinate reference frame as a function of pressure, radius, and area. Assuming the pressure differential across the blade is constant, the complete design is specified by incorporating empirical approximations to supplement the blade loadings and express the analytical relationships in terms of geometric parameters. In addition, a compatible method of centrifugal pump volute design has been formulated by M. V. Duong. It is very important to remember that pump design involves a system; consequently the integral environment of impeller and volute should be considered in the design of each component.

Briefly, NASA turbine pump design is a highly sophisticated mathematical analysis employing the momentum and continuity equations in differential form to formulate the following expressions:

(a) Equations for the derivation of the relative velocity in a direction normal to a streamline.

(b) Equation for blade surface velocity and head rise.

A numerical procedure has been outlined which, when applied intelligently, could produce a pump design based on fundamental fluid mechanics. In addition, some mathematical analysis would have to be made for application of NASA's method to centrifugal pumps. This method assumes a nonviscous media and streamline flow.

The potential flow approach is based on a series of Japanese papers and defines a frictionless, idealized, flow potential function which is substituted into the governing equations of fluid mechanics to obtain expressions involving flow characteristics. The analysis is completely theoretical and employs the theory of straight cascades of thin wings, thin wing lattice theory, etc., to derive the expressions in terms of pump geometry.

The conventional design procedure is the experience-art form of pump design and has traditionally involved the scaling of parameters from operating pumps which closely resemble the operating characteristics of the one being built.

The basic problem with each of the methods outlined above is the lack of experimental evidence to substantiate the dubious assumptions and approximations employed to simplify the analysis. This is especially true in the case of the first three methods. Moreover, information regarding previous results and performance curves of actual pumps designed according to these methods is almost nonexistent.

COMPUTER PROGRAM

The second important aspect of this project is the formulation of a computer program which will help a designer establish pump geometry and essentially free him from the necessity of making trivial and time-consuming calculations. The work to date has consisted of writing a program based on analysis 1. When supplied with head, capacity, and speed of operation, it will define the geometry of the volute casing and impeller. It also will define the blade geometry and overall impeller characteristics. A print-out of the program has been included in the report. An interesting aspect of the computer output is that it will be printed out in graphical form. Additional work is needed before this is entirely satisfactory.

DESIGN

A sketch of an impeller and volute have been made and forwarded to Whirlpool. A working detailed drawing has been made by Whirlpool designer C. Platt, and the prototype is now in their patternshop for fabrication. The volute employs a logarithmic spiral variable circular cross section. Its design is based on a method by Mr. Minh, which is enclosed.

The impeller has been designed using basic modeling laws. It has a 3.4-inch outside diameter and curved variable-height blades. The pump used as a model had an unusually high-efficiency and sound operation and design principles.

A second impeller, based on Dr. Hansen's method, is being made. This originally was to be the first prototype impeller but was held back to incorporate some later design changes. As tests are made the need for additional work and the kind of work required will become apparent. A complete calculation procedure is being prepared along with a computer program to facilitate these calculations.

TESTING

A testing apparatus has been fabricated on the first floor in the Fluids North Campus Laboratory at The University of Michigan. Figure 1 depicts the overall physical characteristics of the test apparatus.

Incorporated in the test apparatus is a magnetic pickup to measure pump speed, a 1/3 horsepower dynamometer to measure reaction torque, an orifice calibrated to determine flow rate, and a pressure manometer to measure head.

A closed circuit was used to run tests on the present Whirlpool combination washer and dryer pump and will be employed to test future prototypes. A closed circuit means that the water in the system completes a cycle, with the amount of water remaining constant, and with water neither being added or removed. The subsequent description will be more readily understandable if Figure 1 is consulted frequently. A reservoir holding approximately twenty-five gallons of water is used as a head tank. From the reservoir, the water flows to the inlet side of the pump. The water is pumped through the pump and discharged into the outlet pipe. Downstream from the pump outlet is an orifice plate and straight pipe where flow rate is measured by the pressure differential depicted on a manometer. Subsequent to the orifice plate is a throttle valve which is used to regulate the flow. From the throttle valve, the fluid enters the reservoir from which it started the cycle. At a given constant speed, all necessary measurements can be taken.

The Whirlpool combination pump has been tested. The pump was determined to be approximately 28% efficient at 3300 rpm. It registered an almost constant head of 27 ft for the entire capacity range. In addition, further tests were run at 3000 rpm and 2470 rpm. A curve of head and efficiency versus capacity as indicated by these tests is enclosed.

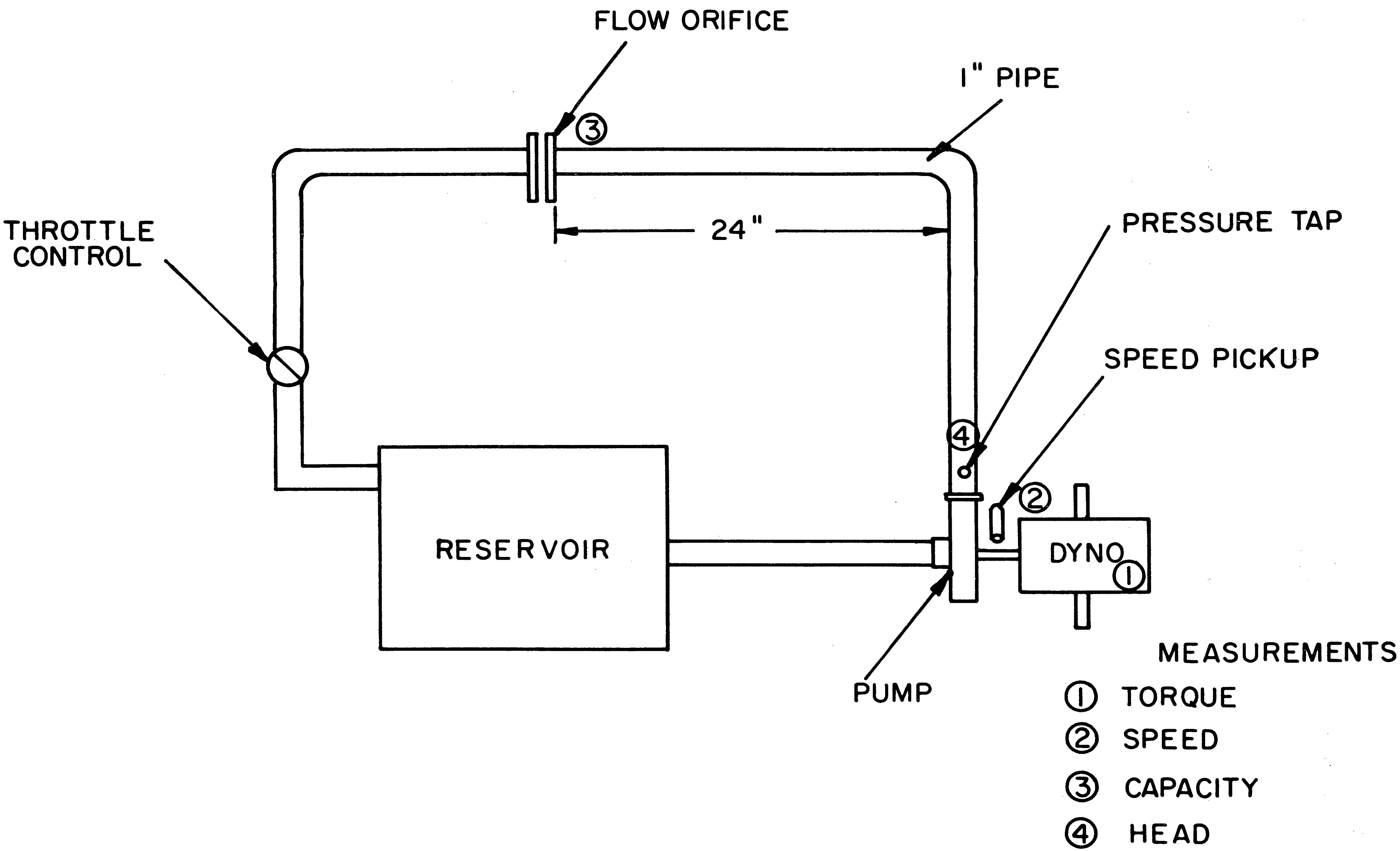

Figure 1. Test flow circuit.

REFERENCES

Peck, J. F., "Investigations Concerning Flow Conditions in a Centrifugal Pump, and Effect of Blade Loading on Head Slip," English Society of Mech. Engrs., April 1950.

Addison, H., "Centrifugal and Other Rotodynamic Pumps," Chapman and Hall, London, 1955.

Kovats, A., "Design and Performance of Centrifugal and Axial Flow Pumps," Wiley, New York, 1957.

Csanady, G. T., "Theory of Turbomachines," McGraw-Hill, New York, 1964.

Church, A., "Centrifugal Pumps and Blowers," Wiley, New York, 1929.

Stepanoff, A. J., "Centrifugal and Axial Flow Pumps," Wiley, New York, 1957.

Murata, S., "Research on the Flow in a Centrifugal Pump Impeller," Six reports in all, Bulletin of JSME, 1960.

Acosta, A., and R. Bowerman, "An Experimental Study of Centrifugal Pump Impellers, ASME Paper No. 56-A-41, 1957.

Final Report, Project P502, NASA

Lichtenstein, J., "A Method of Analyzing the Performance Curves of Centrifugal Pumps," ASME Paper No. HYD-50-3, 1927.

AN INVESTIGATION OF A POWER SYSTEM FOR OPERATING A ONE-HORSEPOWER, BRUSHLESS, 18,000 RPM ELECTRIC MOTOR

Gee-In-Goo

The purpose of this research project is to investigate means of developing a system for operating a one-horsepower, brushless, 18,000 rpm electric motor from the normal 115-volt, 60-cycle, household supply.

An extensive survey of the literature indicates that several systems have been developed for changing line frequency to some multiple of line frequency, generally to two or three times line frequency. However, we could discover no indication that any of these systems had been used to develop a high-frequency supply of large power capacity. Although some limited-capacity multipliers use a single-phase source, the most successful frequency multipliers require a polyphase source.

Inasmuch as our system must operate from the 60-cycle, 115-volt supply, we have spent considerable time attempting to develop a frequency multiplier that will produce at least 1,000 watts at 300 or 360 cycles. While we were able to multiply the frequency, we were unsuccessful in our attempts to develop sufficient power within reasonable limits of voltage regulation. We shall discuss this system in detail later in the paper.

Trade and technical literature was investigated to determine the commercial availability of ac and dc motors which would operate in the 18,000 rpm speed range. One-horsepower or larger ac motors which operate from a power source with a frequency of 400 cps and at efficiencies which are comparable to those of 60-cycle motors are available. Thus, a motor which would fill our needs is commercially available if we can develop a suitable frequency multiplier to be used with it.

We also found in the trade and technical literature several references to high-speed, brushless, dc motors. One of these is the Kenletro motor by Lam Electric Division of Ametek, Incorporated. Its circuit diagram (Figure 1) shows that it utilizes the feedback principle. This motor is of fractional (1/10) horsepower and 18,000 rpm. Lam Electric is trying to develop larger capacity motors which will employ this same principle, but to date their attempts have been unsuccessful. Haydon Switch and Instrument, Incorporated, also makes a series of commercially available brushless, dc motors. However, these are in the hundredth of a horsepower range. The company's diagram (Figure 2) indicated that they are synchronous motors, which utilize a permanent magnet and a varying field winding with a transistorized switching circuit. A maximum speed of 6,000 rpm is indicated in the literature.

There have been two similar developments of brushless, dc motors, one by Goddard Space Flight Center, Maryland (Ref.1), and another by Philip A. Studer of NASA, NASA-TN-D-2819 (Ref. 2). Both use a set of diodes which are controlled by photo cells. When light is shined on a light-sensitive element, a potential difference is generated across its terminals. This potential, in

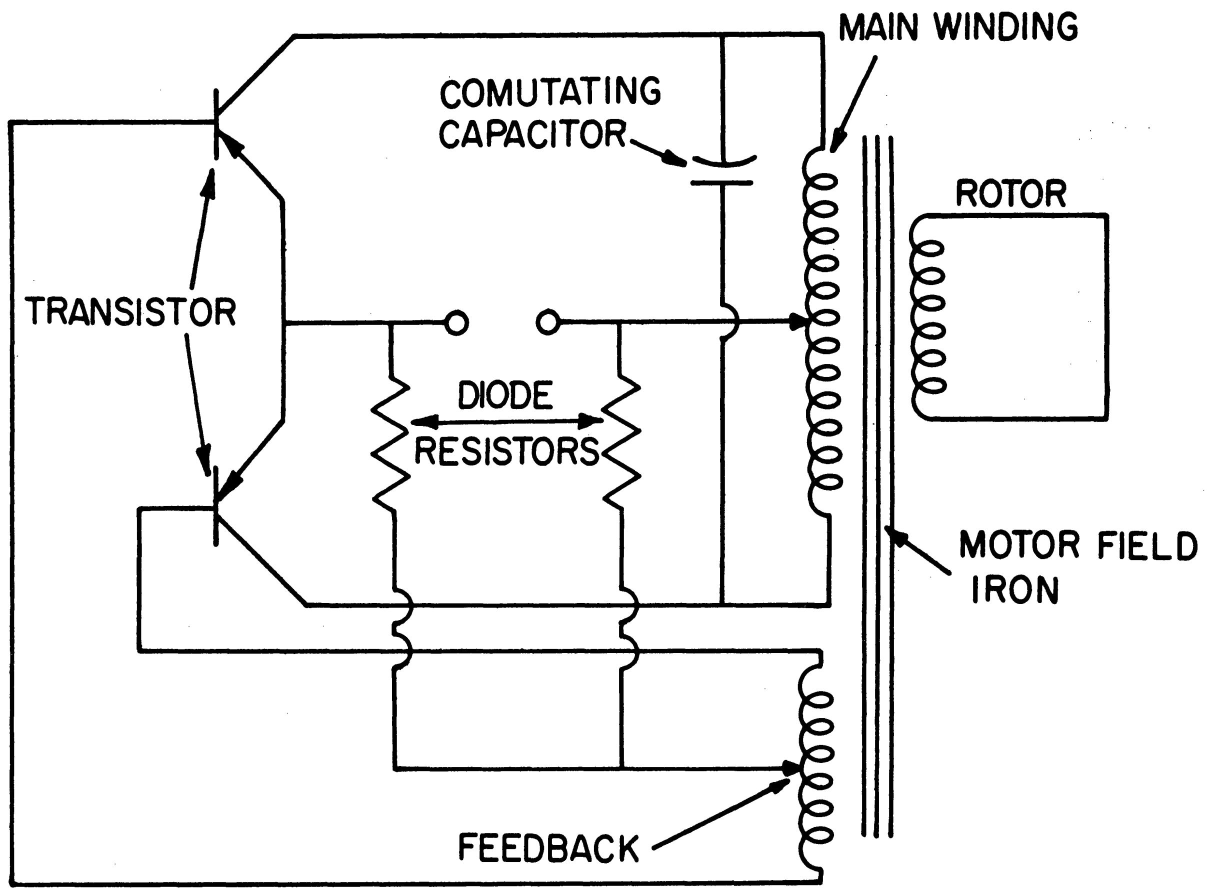

Figure 1. Kenletro motor circuit diagram.

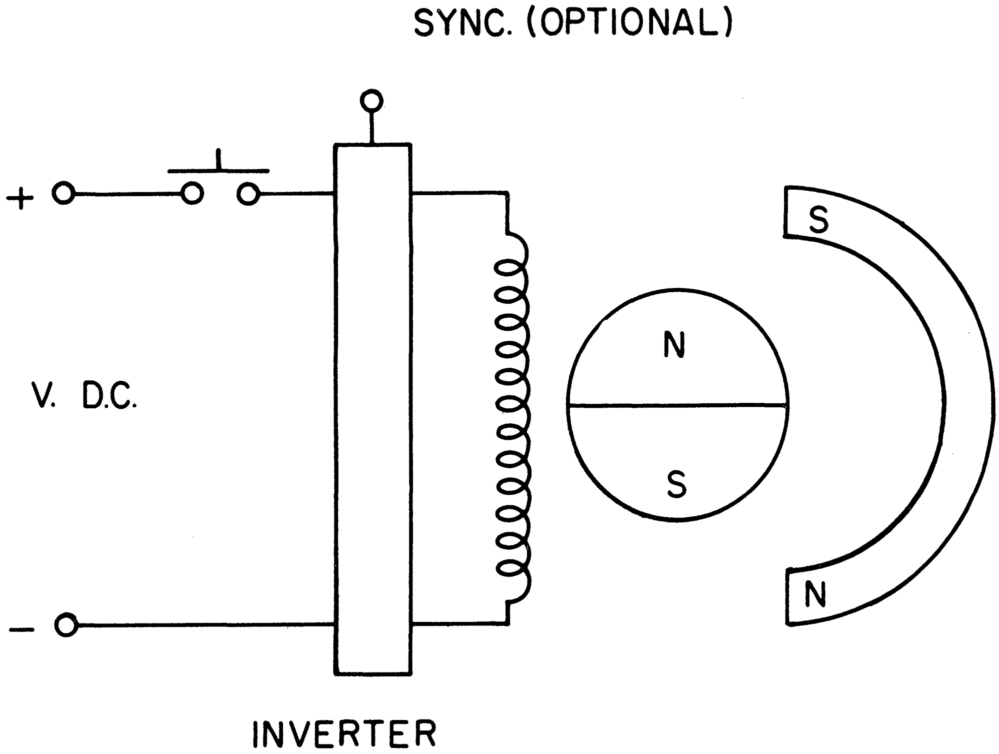

Figure 2. Brushless dc motor wiring diagram.

turn, controls the diodes. A device is mounted on the shaft of the motor to regulate the light that shines on the photo cells. These are fractional horsepower motors. Essentially, they are ac motors in that the diodes are inverting dc to ac power. The developers feel that these motors could be scaled up to deliver more power and higher speed. However, our experience indicates that this is easier said than done. In order to apply this method to our project, we would have to rectify ac to dc and then invert dc back to ac. Our discussion of transistorized elements later in this report will indicate why it is not feasible to rectify ac to dc and then convert dc back to ac for larger power applications.

Mr. A. Tustin of the Imperial College of Science and Technology, London, has developed a method of replacing the commutator with switching devices, such as controlled silicon rectifiers (Ref. 3). His is an excellent method of eliminating the commutator. However, a study of his circuit diagram (Figure 3) indicates that the motor speed is governed by the frequency of the input power. To make use of this method for our project, we would need a 300 cps power supply. If we had a 300-cycle supply, we could use an ac motor.

The Japanese also have done research on commutatorless motor which they describe as a polyphase (3-phase), synchronous motor equipped with SCR inverters. Pulses are fed from a distributor, which is mounted on the shaft, and which detects the motor position and speed. It is reported that this motor has difficulties due to the higher harmonics in the pulse. Higher harmonics either lead or lag the rotating field, thereby causing parasitic torques and high-frequency losses in the rotor. Thus, use of silicon control rectifiers, SCR, introduce new problems, which will be discussed later.

We have considered the electronic circuits, such as the R-C or the L-C oscillators, which enable one to change the input frequency to a higher frequency by selecting the proper value of R, L, and C components. We found that 300 cps or 360 cps is a relatively low frequency in electronic circuitry. The value of capacitance and inductance would have to be relatively large. It is inconvenient to have both ac and dc power in our system, because the dc power would have to be rectified from ac input. Also the efficiency of electronic circuits is relatively low. If we were to use flip-flop circuits or flasher-type circuits, we would run into the problem of higher harmonics again. Therefore, we feel it is impractical to apply electronic circuits to this project because of the relatively large amount of power required.

Let us consider the properties of transistors. From a rough calculation, we estimated that the system needs to produce approximately 1000 watts of power. The fact that our supply voltage is 115 volts means that the current must exceed 10 amperes since the power factor will be less than unity. Transistors of this capacity generally have 80 to 100 watts of power dissipation each. This would require that more power be supplied to the system. In addition, at present, power transistors are not highly dependable. In the case of the Japanese "Sakuma Frequency Converter Project I" (Ref. 5), the frequency

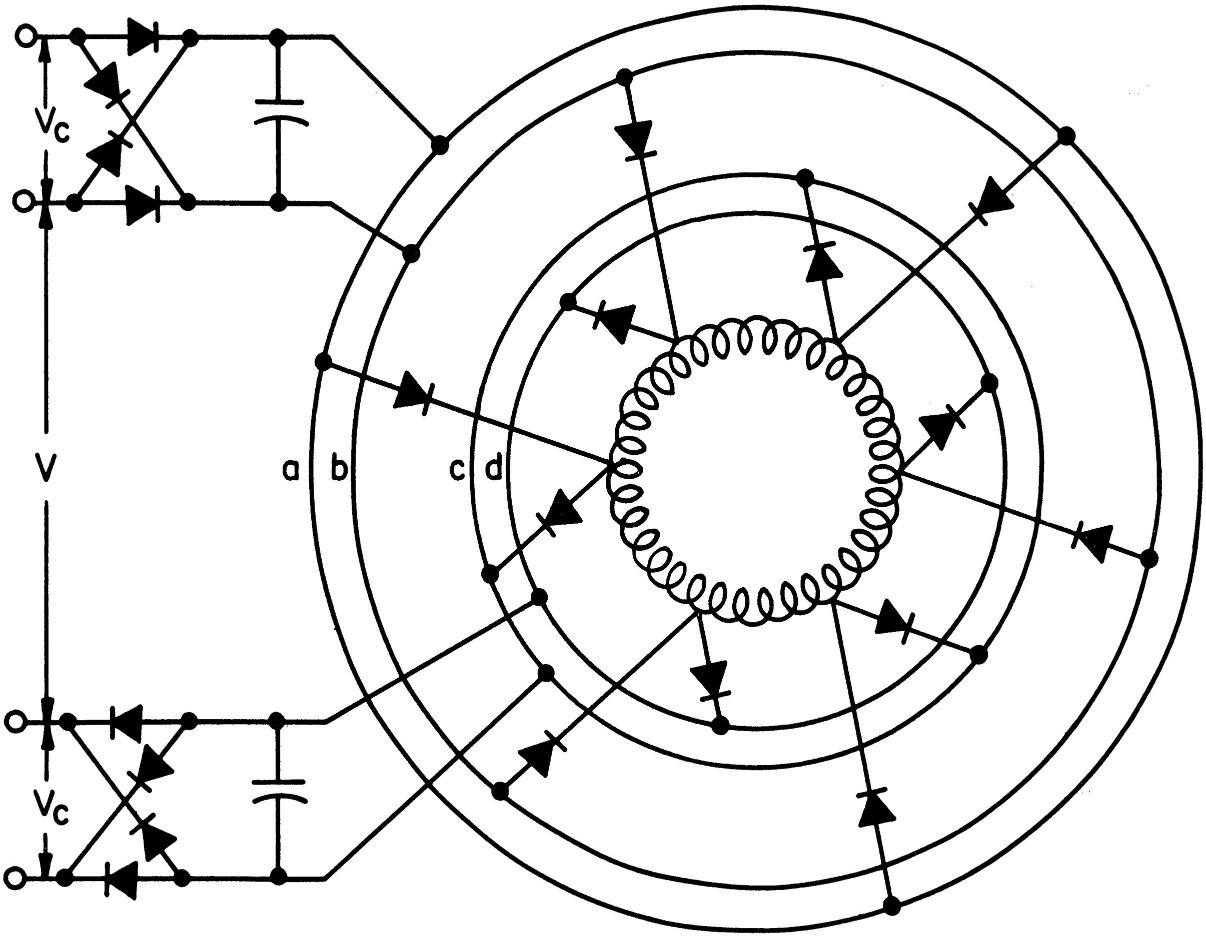

Figure 3. Commutating circuit diagram.

change is accomplished by the electron tube circuits.

After considerable study, and after having given much thought to the project, we have concluded that ac motor drive is superior to dc motor drive. Thus, we have concentrated our efforts on the development of an ac system. Once we have designed an adequate system, we believe that we can obtain a motor to meet the required specifications. However, while we have spent most of our time trying to develop a frequency multiplier, we have also considered the dc motor briefly. It may be feasible to eliminate brush wear by using liquid metal, such as mercury or a sodium alloy. A homopolar dc motor may have possibilities. Further research and experimentation will be necessary before we can come to any conclusions relative to the use of a dc motor on this project.

After careful study of these different methods, we feel that the frequency transformer may be a solution to our problem. The frequency transformer operates on the highly nonlinear region of the hysteresis curve or by polarization of the magnetic core. The major developmental work on frequency transformers, which has been done by the Russians, has involved the use of a polyphase power source. There are a few which use the single-phase source, although these were only briefly described.

We have considered both the frequency tripler and the frequency doubler. A frequency tripler is made up of two transformers (Figure 4). It makes use of the nonlinear property of the hysteresis curve. When transformer I is highly saturated, it generates the higher harmonics, mainly the third harmonic, in the applied current because of the nonlinear effect of the hysteresis curve. Transformer II is kept from saturation by an air gap. The high reluctance of the air gap prevents the core from being saturated. As shown in Figure 4, the primaries of both transformers are connected in series. Therefore, the current applied to transformer I, which carries the third harmonic, is also applied to transformer II. As a result, the third harmonic exists in both transformers (Figure 6), and they are 180° out of phase. If one were to connect the output of the transformers with opposing polarity, as shown in the diagram, one would find that the amplitude of the fundamentals cancel each other while the third harmonic amplitudes add. Thus, one would obtain an output voltage consisting of mainly the third harmonic, a frequency three time that of the fundamental.

A frequency doubler also consists of two transformers (Figure 7). However, it uses the polarization method to magnetize the core of the transformer in one direction or the other. Since the flux density in the core of a transformer follows the waveshape of the applied voltage, which is sinusoidal in our case, the polarization causes the sinusoidal flux density to be distorted. The distorted sinusoidal wave could be resolved into two frequency waves, the fundamental and its second harmonic. Again, by connecting the output of the transformers with opposing polarity, one could obtain the second harmonic of the fundamental. The fundamentals cancel out very nicely.

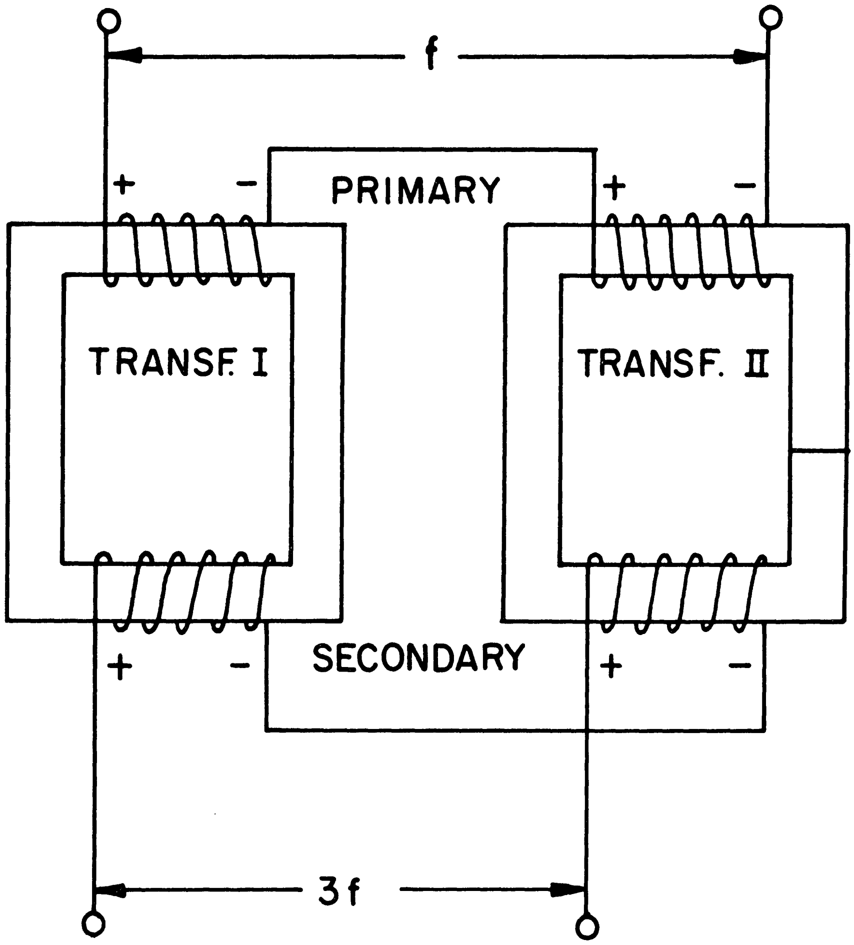

Figure 4. Frequency tripler circuit diagram.

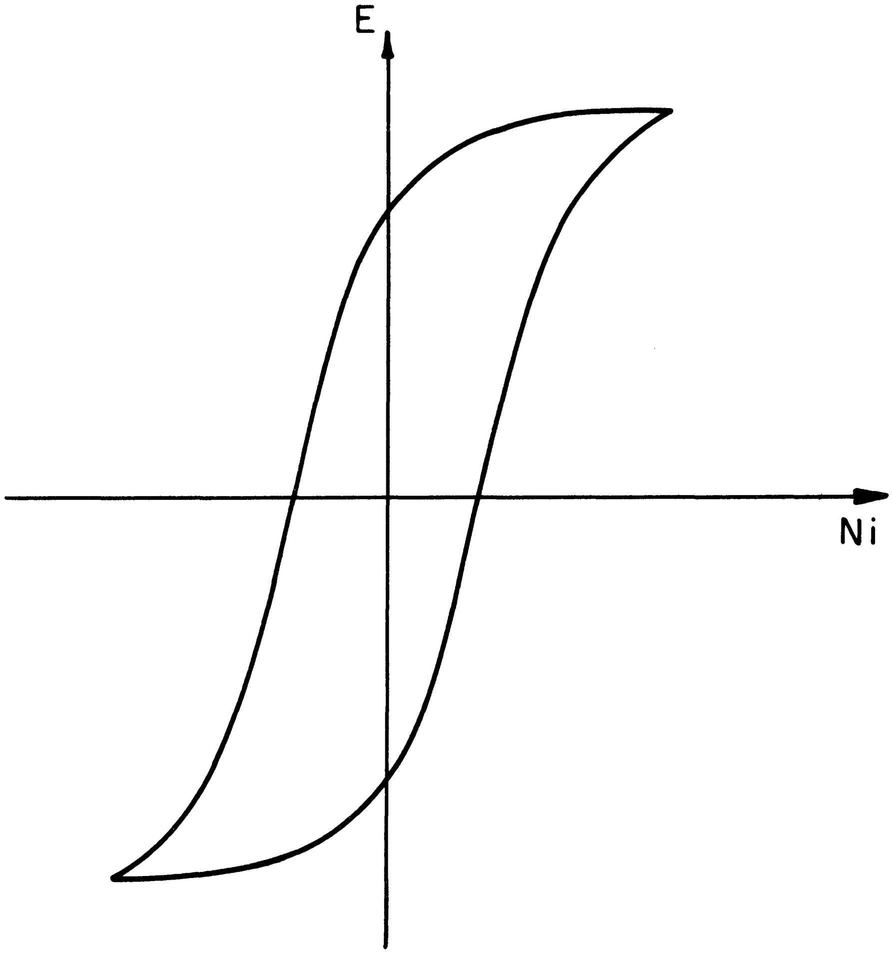

Figure 5. Hysteresis curve.

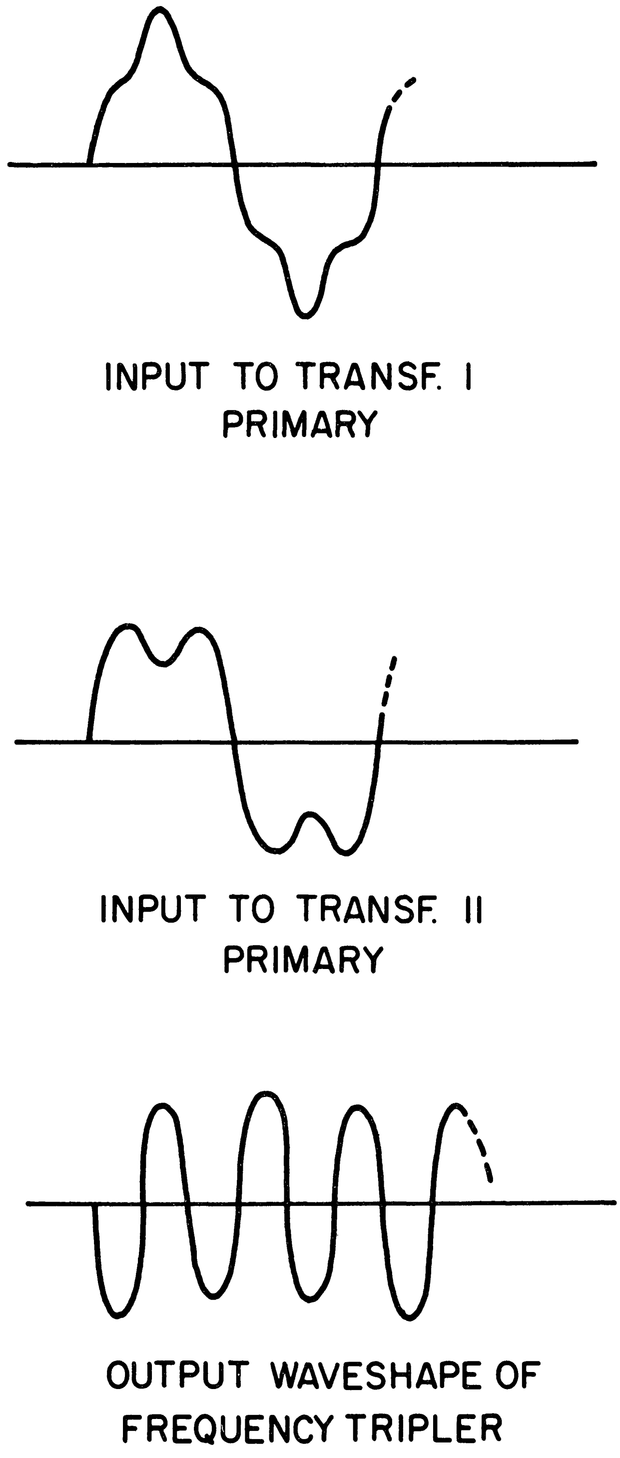

Figure 6. Transformers

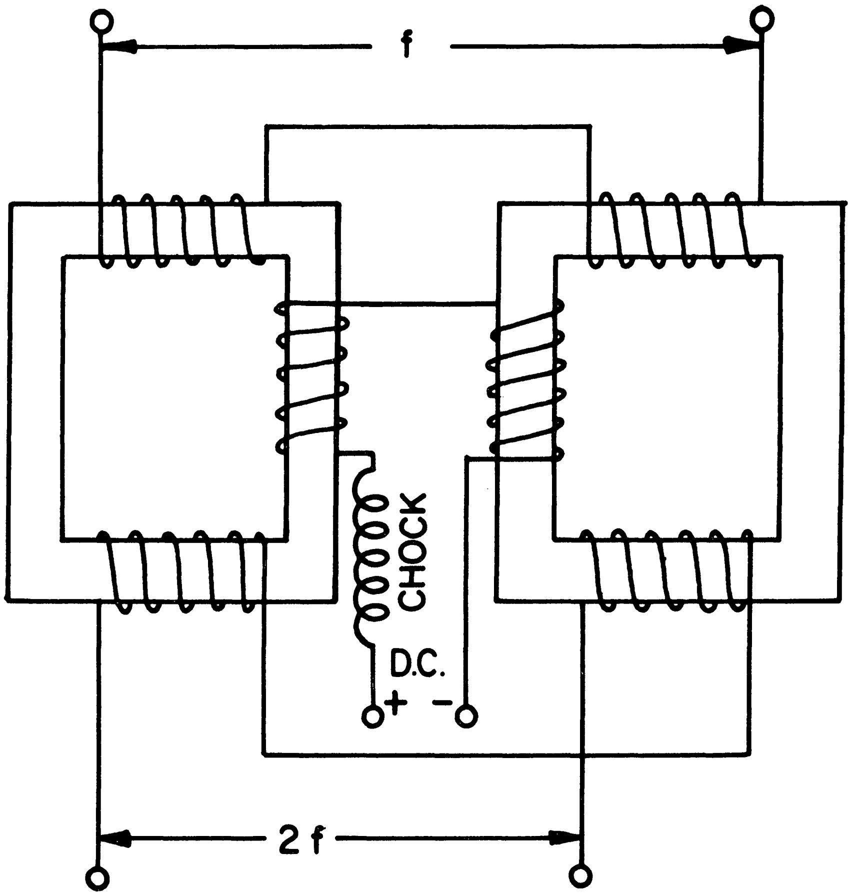

Figure 7. Frequency doubler circuit diagram

If these frequency multipliers are successful, two frequency multipliers could be cascaded together to obtain the desired frequency. By cascading two doublers together, one could obtain the fourth harmonic (240 cps) of the fundamental. By cascading a doubler with a tripler, one could obtain the sixth harmonic (360 cps). The cascading of two triplers would multiply the fundamental nine times (540 cps).

We did some preliminary testing of the frequency doublers and frequency triplers. With the doubler, we observed the second harmonic of the fundamental, and with the tripler we observed the third harmonic of the fundamental. A 100 VA transformer was converted into a variable air core transformer for further testing of the frequency tripler.

We determined the length of the air gap required to give us a third harmonic with a minimum fundamental superimposed on it. The required length is only 0.001". The data we obtained from testing with a unity power factor (resistive) load were not as good as we would have liked. For both frequency changers, the data show a poor voltage regulation and low efficiency. After careful analysis of these results, we feel that they could be improved. However, we are not prepared to estimate by what factor we could improve the results.

The following analysis leads us to believe that the frequency changers could be improved. Let us consider the frequency tripler. First, the transformers used for these testings were designed for the 60 cps power source. When the third harmonic is applied to the transformer, the impedance of the transformer goes up nearly three times, because the frequency has tripled. Second, if the fourier analysis of the resulting wave is considered, it is found that the third harmonic is but a third of the amplitude of the fundamental. This accounts for the low-voltage and low-power output of the frequency tripler. Because the ordinary transformers are not designed to operate in the highly nonlinear region of the hysteresis curve, one could not saturate the transformer core as much as one would like. Also, when power is being drawn from the secondary of the transformer, a back emf tends to oppose the magnetization of the transformer core. This causes the transformer core to be less saturated. As a result, the frequency tripler has very poor voltage regulation. If the transformer core of the frequency multiplers could be kept highly saturated, they might have a better voltage regulation. A similar result was obtained from the frequency doubler. Because the frequency tripler could only transfer limited power, we were not able to test it with a motor. However, the doubler that we tested was able to drive a 1/8 horsepower motor at twice the rated speed.

We feel that there are many ways to improve the frequency changers. One could begin with the impedance of the transformer, that is, redesign the transformer for the desired frequency operation. This would probably improve the efficiency of the transformer. Secondly, one could design a transformer to be operated on the highly nonlinear region of the hysteresis curve. The iron core transformer and the air core transformer would have to be designed so that the voltage division at the primary of both transformers would be more desirable. At present, the voltage division of the iron core transformer is twice that of the air core transformer. Also, the output voltage of the iron core transformer is three times that of the air core transformer. We feel the voltage division at the primary should be a one to one ratio. This could be accomplished by changing the impedance ratio of the respective transformers. Professor Carey feels that a change of transformer core material might also improve the results.

REFERENCES

1. Development of a Brushless D. C. Motor, Goddard Space Flight Center, Md.

2. Studer, A. P., Development of a Sealed Brushless D. C. Motor, NSAS-TN-D-2819.

3. Tustin, A., Electric Motor in Which Commutation is By Switching Devices Such as Controlled Silicon Rectifiers, Imperial College of Science and Technology, London, September 4, 1963.

4. Miyashi and Tunehiro, Research on the Commutatorless Motor with Silicon Controlled Rectifier.

5. "Sukuna Frequency Converter Project I," Power Apparatus and System, 84, May 1965, pp. 411-415.

BIBLIOGRAPHY

Books

Alley, C. L., and K. W. Atwood, Electronic Engineering, Wiley.

Fitzgerald, A. E. and C. Kingsley, Electric Machinery, McGraw-Hill, 1961.

Rozhankii, L. L., Static Electromagnetic Frequency Transformers, Pergamon, 1963.

Ryan, Design of Electrical Machinery: D.C. Dynamos.

Still, Principles of Electrical Design, McGraw-Hill.

Stout, M. B., Analysis of A.C. Circuit.

Papers

Black, L. R., "The Frequency Tripler," Proc. IEEE 100, Part II, No. 75, 1953.

Cleminson, C. A., Static Regenerative Variable Frequency Devices.

Downie, E. G., "Magnetic Frequency Multiplier for Fluorescent Lighting," Electronics, 1955.

Kantwell, "Frequency Tripling Transformers," Trans. AIEE, 55, No. 7, 1936.

Miyashi and Tunehiro, Research on the Commutatorless Motor with Silicon Controlled Rectifier.

Parker, Analytical Methods for Permanent-Magnet Design, General Electric Company, Edmore, Michigan.

Schiff, A. N., Semiconductor Devices.

Studer, A. P., Development of a Sealed Brushless D.C. Motor, NASA-TN-D-2819.

Tustin, A., Electric Motor in Which Commutation is By Switching Devices Such as Controlled Silicon Rectifiers, Imperial College of Science and Technology, London, 4 September 1963.

Williams, F. G. and S. W. Noble, "The Fundamental Limitations of the Second Harmonic Type of Magnetic Modulator as Applied to the Amplification of Small D.C. Signal," Proc. IEEE, 97, Part II, 1950.

Solid-state Components in Sparkless Motor, and in Controls for Motor of Furnace Blower.

"Sakuna Frequency Converter Project I," Power Apparatus and System, 84, May 1965, pp. 411-415.

Development of a Brushless D.C. Motor, Goddard Space Flight Center, Md.

AN INVESTIGATION OF THE DESIGN PARAMETERS OF
THE CONDENSER AREA IN AN EXTRACTION DRYER

Vern Wedeven

DEFINITION OF SYMBOLS

$\Delta\ p_L$ = change in pressure of liquid phase

$\Delta\ p_G$ = change in pressure of gas phase

ρ = density

f = friction factor

L = length

V = velocity

D = diameter

g = acceleration of gravity (32.2 ft/sec^2)

DEFINITION OF PROJECT

This report concerns that part of the extraction system where the flow of fluid leaves the cylinder and passes through the extraction nozzle, condenser, and suds trap. The purpose of this project is to ascertain the significant design variables involved, to determine the relationships between them, and, thus, to facilitate the development of a mathematical model that can be incorporated with a computer to achieve an optimization of the design variables. The project should provide the engineer with not only a theoretical analysis of the system, but also an understanding of the principles involved.

FLUID FLOW THROUGH SYSTEM

The basic function of the nozzle, condenser, and suds trap is the transportation of fluid. The criteria for an optimum design of these components may include some or all of the following:

1. Pressure drop.
2. Flow characteristics for efficient condensation and/or phase separation.
3. Dynamic response between blower and cylinder.

The design parameters involved include: diameter, length, friction, factor, and shape.

The relative importance of each of the above design criteria has not yet been determined. However, pressure drop is an ever-present effect and its origin and method of determination should be understood.

SINGLE-PHASE FLOW

Pressure drops for single-phase flow present no particular problems and are usually handled by the following equations:

For straight pipe

$$\Delta p = \frac{\rho f L V^2}{2\ gc\ D} \tag{1}$$

For change in flow direction

$$\Delta p = K \frac{\rho V^2}{2\ gc} \tag{2}$$

where K is a constant determined from the magnitude of band (K = .9 approximately for a 90° turn). These equations are for incompressible flow and can properly be applied to the fluids in our system. The density changes in air, for example, do not become important for engineering calculations until its flow speeds reach a Mach number of .3. The estimated Mach number in our system is not expected to exceed 0.15.

If one applies Eqs. (1) and (2) for a single-phase flow of air, the resulting pressure drops are small. A pressure drop of .004 in. of water was calculated for a straight duct, which reflects the negligible effect of wall friction. Wall friction seems to be important only for long pipelines or extremely rough surfaces, neither of which we have. The pressure drop across the suds trap is on the order of .7 in. of water, which reflects the energy loss due to viscous shear during its momentum change.

TWO-PHASE FLOW

It would be a mistake to consider only a single-phase flow of air in the determination of pressure drop. The fact that air, water, and water vapor are simultaneously flowing in our system to greater or lesser degrees complicates our problem. However, the problem can be reduced to that of two-phase flow if one considers the water as a liquid phase and the air and/or water vapor as a gas phase. To handle two-phase flow problems it is necessary to combine some analytical methods with some experimental results. A striking characteristic of two-phase flow is that the phases do not move at the same velocity, particularly at low pressures. The gas phase usually moves more rapidly. When two phases flow in a horizontal duct, they can be distributed in the duct in a number of different configurations, and the analysis of any two-phase flow problem begins by specifying the flow pattern.

If a constant liquid rate is maintained in a horizontal pipe and the gas rate is gradually increased from zero gas rate to higher values, the following sequence of flow patterns may be observed.

1. Bubble Flow, characterized by individual gas bubbles moving along upper section of pipe.

2. Plug Flow, with characteristic plugs resulting from the coalescence of gas bubbles.

3. Stratified Flow, in which complete segregation of gas-liquid phases occur with upper portion of pipe filled with gas phase.

4. Wave Flow, in which interface between gas and liquid becomes unstable and waves form.

5. Slug Flow, in which, at higher gas rates, the amplitude of the waves grow large enough to bridge across the top of the pipe.

6. Semi-Annular Flow, in which surface tension causes liquid phase to confine itself in an area adjacent to the pipe and the gas phase passes through the annular ring formed by the liquid.

7. Spray Flow, in which increase in gas flow rate is so large that the liquid phase becomes dispersed in the gas phase.

Martinelli (Ref. 1) is the prime contributor to two-phase flow problems. He subdivides flow patterns into four classes, called "Flow Regimes," based on whether the gas and liquid phases have turbulent or laminar flow. If the individual liquid and gas flow rates, diameter and length of duct, viscosity and density of each phase are known, the pressure drop can be determined by the following basic steps.

1. Assuming that liquid and gas phases are flowing alone, calculate single-phase pressure drops for both liquid and gas phases. Equation (1) can be used for this.

2. Calculate an X parameter defined as

$$X = \sqrt{\frac{\Delta p_L}{\Delta p_G}} \tag{3}$$

3. Calculate Reynolds number for both phases as if they were flowing separately. In this step, one must determine the degree of "hold up" which is defined as the volume fraction of pipe occupied by one of the phases present in the flow system. Based on the Reynolds number, the Flow Regime is determined.

4. Using the X parameter and Flow Regime, a ϕ parameter and the pressure drop calculated from either one of the phases., eg.,

$$\left(\frac{\Delta p}{\Delta L}\right)_{\substack{\text{Two} \\ \text{Phase}}} = \phi^2_{\text{Liq.}} \left(\frac{\Delta p}{\Delta L}\right)_{\substack{\text{Liq.} \\ \text{Phase}}} \tag{4}$$

A hypothetical problem was solved using the Martinelli method. It appears that the pressure drop resulting from the relative velocity difference between the two phases is indeed significant in comparison with a single-phase pressure drop. The Martinelli method provides insight into the principles and mechanisms of two-phase flow that could assist an engineer in design. However, due to the complex nature of two-phase flow, the Martinelli method seems to be most applicable to flow problems in which the physical geometry is simple (horizontal or vertical pipes), and in which the flow is steady.

In summary, then, the pressure drop in the system under consideration seems to result from:

1. Wall friction
2. Viscous shear in fluid during momentum changes
3. Velocity differences in two-phase flow

One hesitates to make conclusions about the general work considered thus far; however, the following might be said about pressure drop. The effect of wall friction should be small because of the relatively smooth surface used and the short duct lengths involved. Effects of velocity differences in two-phase flow may be significant particularly where the flow inclinations become nearly vertical. The effect of shear in the fluid during momentum changes may also be significant depending upon geometry.

SPRAY CONDENSER

The primary thermodynamic function of the area under consideration is that of condensation. The spray condenser seems to be an almost ideal component for this function and offers the following advantages.

1. Good cooling surface contact
2. Simple construction
3. No tube fouling
4. Condenser water removes lint from system and acts as a cleaning agent by removing dirt particles out of the air.

The spray condenser, though simply constructed, presents many complications in its element description as compared with a conventional heat exchanger. It becomes indeed a bit sticky when one is to determine the area of contact and heat transfer coefficients between the cooling water and the air-vapor mixture. Also, the unsteady nature of the drying process does not make analysis any simpler. Recognizing the difficulties involved, one is forced to make simplifications of the problem and to proceed with an objective of providing as complete an analysis as possible from the theoretical viewpoint.

CONDENSATION PROCESS

The importance of condensation cannot be overemphasized since the performance of the process will directly influence the drying efficiency of the entire system. It is important, therefore, to understand well the mechanisms and parameters involved.

Condensation involves a simultaneous rate process of heat and mass transfer. Consider, first of all, the mass transfer in a drop of cold water surrounded by hot, moist air. Molecules of water continually diffuse from the surface of the drop and form a vapor film around the water droplet. The partial pressure of this vapor film varies directly with the temperature of the water droplet. The water vapor in the moist air also has a partial pressure which varies directly with its temperature. When the partial pressure of the water vapor in the humid air is greater than the partial pressure of the water vapor surrounding the water droplet, transfer of water vapor occurs from the moist air to the water vapor film around the water droplet. This mass transfer, or condensation, will continue until the temperature of the moist air is reduced and the temperature of the water droplet is increased to the values at which their partial pressures are equal.

The rate of mass transfer, or condensation, depends on a driving potential (difference in partial pressures) and a resistance. This can be expressed by the following equation (Ref. 2):

$$\frac{dm}{dt} = KA\,(p_{va} - p_{vw})$$

where $\frac{dm}{dt}$ = rate of vapor diffusion

K = diffusion coefficient or resistance

A = surface area of water droplet

p_{va} = partial pressure of water vapor in air

p_{vw} = partial pressure of water vapor surrounding the water droplet

This equation is not very practical, since the surface area of a water droplet may be difficult to evaluate; however, it does show the relation between the variables involved.

A rate process of heat transfer also occurs in condensation in which heat is removed from the air by the cooling water. Heat is first transferred by conduction from the hot air to the cold vapor film surrounding the water droplets (called "sensible heat transfer"). The rate of heat transfer is determined by the temperature difference and the heat transfer coefficient of the air-water vapor phase. Secondly, latent heat of condensation is transferred to the water droplets from the gas-liquid interface. The rate of heat transfer is directly proportional to the mass transfer during condensation and is determined by the amount of water condensed and its latent heat of condensation at that particular temperature. An equation can be developed if one realizes that the heat transferred across a water droplet surface must be equal to the heat transferred across the vapor film surrounding the droplet plus the latent heat given up at the gas-liquid interface on condensation of the mass transferred across the gas film. For heat transferred across a unit surface we have (Ref. 3):

$$h_L \; (T_i \; T_L) \; = \; h_G \; (T_G \; T_i) + \lambda k \; (Y_G \; Y_i)$$

where T_i = temp. at gas-liquid interface

T_L = temp. in water droplet

T_G = temp. in air-water vapor phase

h_L = water-phase heat transfer coefficient

h_G = gas-phase heat transfer coefficient

k = gas-phase mass transfer coefficient

Y_i = abs. humidity of air at interface

Y_G = abs. humidity of air in gas phase

λ = latent heat of condensation

Again, this equation is not very practical, although it does show the relation between some of the variables involved.

The mechanism of condensation involves both sensible and latent heat transfer. Therefore, it would seem reasonable that the enthalpies of the air and water should be used to postulate driving forces and changes in fluid conditions, rather than using humidity and temperature alone. Considering the air, vapor, and condensed water as a thermodynamic system, the first law of thermodynamics can be used for analysis. Considering steady state and one lb of dry air, the first law states (Ref. 4)

$$g + h_1 + \frac{V_1}{2\ gc} + \frac{g}{gc} Z_1 = h_2 + \frac{V_2^{\ 2}}{2\ gc} + \frac{g}{gc} Z_2 \tag{7}$$

There is no work done on or by the system. Assuming the difference in height and change in air velocity to be small between inlet and outlet, the kinetic and potential energies can be neglected. The simplified relation follows:

$$q + h_1 = h_2 \tag{8}$$

To handle the change of phase in our system, let

W_{T1} = mass of vapor entering per lb of dry air

W_{T2} = mass of vapor leaving per lb of dry air

$W_{T1} - W_{T2}$ = amount of water condensed per lb of dry air

The first law then becomes

$$q + h_{a1} + W_{T1}\ h_{v1} = h_{a2} + W_{T2}\ h_{v2} + (W_{T1} - W_{T2})\ h_{\ell 2} \tag{9}$$

or

$$g = h_{a2} - h_{a1} + W_{T2}\ h_{v2} - W_{T1}\ h_{v1} + (W_{T1} - W_{T2})\ h_{\ell 2} \tag{10}$$

where

q = heat transferred to water

h_{a1} = enthalpy of air entering

h_{a2} = enthalpy of air leaving

$W_{T1}\ h_{v1}$ = enthalpy of water vapor entering

$W_{T2}\ h_{v2}$ = enthalpy of water vapor leaving

The heat transfer represented by the above equation must be absorbed by the cooling water. It, too, goes through an energy change that can be represented by the first law.

$$q_W = h_{T2} - h_{TW1} \tag{11}$$

Eqs. (10) and (11) can then be combined.

$$h_{T2} - h_{TW1} = h_{a2} - h_{a1} + W_{T2}\, h_{v2} - W_{T1}\, h_{v1} + (W_{T1} - W_{T2})\, h_{\ell 2} \tag{12}$$

In summary, we have found that condensation occurs when the partial pressure of the water vapor in the air becomes greater than the partial pressure of the water. Thus, by increasing the temperature of the inlet air, and thus its vapor pressure, and decreasing the temperature of the inlet cooling water, and thus its vapor pressure, a greater rate of condensation will occur.

COMPUTER ADAPTION

The solution of the first law can provide the relative variations between many of the parameters involved. Its incorporation into the computer, however, requires several idealizations and assumptions. Although our mathematical description may now deviate from the real system, it is felt that the information received will provide greater insight into the characteristics of the condensation process. Refinements of the description that will lessen the deviations between the theoretical and practical can be made after a full development and understanding of the idealized approach. The first law establishes the thermodynamic boundaries or limitations of the real system. It sets up regions within which we know the system will operate.

To calculate the exit conditions for various inlet conditions, using the first law, the following assumptions were made:

1. Equilibrium conditions—Condensation involves the rate processes of heat and mass transfer. Assuming time for equilibrium of both processes, the exit cooling water and air-vapor mixture will be at the same temperature. This establishes an upper bound on the amount of heat transferred to the cooling water and the amount of water condensed.

2. Saturation process—The inlet relative humidity as well as its variation through the drying cycle is now known. The assumption of 100% relative humidity establishes the boundary of the maximum amount of water vapor that can enter the condenser at a particular temperature.

3. Steady State Process

4. No External Heat Transfer

5. Constant Specific Heats

The first law in the form of Eq. (12) can be solved for various temperatures by using gas tables to obtain the enthalpies of air, and steam tables to obtain the enthalpies of the two water phases (saturated liquid and vapor). The humidity ratio (W) for particular temperatures can be obtained from the psychrometric chart.

It would be difficult, however, to provide the computer with all the information contained in the psychrometric chart, gas and steam tables. A mathematical approach whereby the computer calculates the enthalpies and humidity ratios as needed has greater appeal. The enthalpies can be calculated by using the perfect gas relation

$$h = C_p T + \text{constant}. \qquad (13)$$

Using average values of constants and specific heats between 100°F and 200°F, Eq. (12) becomes

$$\begin{aligned} &MCW\,(T2-TW1) = MA\,\{-.241(T2-T1)-W_{T2}[.407(T2+460)+877.6] \\ &+W_{T1}[.407(T1+460)+877.6]-(W_{T1}-W_{T2})[(T2+460)-492.53]\} \qquad (14) \end{aligned}$$

where

T1 = inlet air-vapor temperature, °F

T2 = outlet air-vapor temperature, °F

MA = dry air flow rate, lb/min

MCW = cooling water flow rate, lb/min

W_{T1} = humidity ratio for inlet temperature, $\dfrac{\text{lb of vapor}}{\text{lb of dry air}}$

TW1 = inlet cooling water temperature, °F

The determination of the humidity ratio presents a more difficult problem, for there seems to be no direct mathematical approach available. An empirical relation developed by Smith, Keys, and Gerry gives the vapor pressure of water for particular temperatures.

$$\mathrm{LOG}_{10} \frac{p_c}{p_v} = \frac{x}{T} \left[\frac{a' + b'x + c'x^3}{1 + d'\ x} \right] \tag{15}$$

where

p_v = vapor pressure of water in int. atm.

p_c = 218.167 int. atm.

T = $t(°C) + 273.16$

x = $(T_c - T)$ $\qquad T_c = 647.27$

a' = 3.2437814

b' = 5.86826×10^{-3}

c' = 1.1702379×10^{-8}

d' = 2.1878462×10^{-3}

The above equation also applies to the vapor pressure in the air, since equilibrium of the condensation process occurs when the vapor pressure of water equals the vapor pressure in the air. Using this vapor pressure, the humidity ratio can be calculated by the following derivation.

$$W = \frac{\text{mass of vapor}}{\text{mass of air}} = \frac{m_v}{m_a}$$

$$m_v = \frac{p_v\ V\ M_v}{\bar{R}\ T} \qquad\qquad m_a = \frac{p_a\ VM_a}{\bar{R}T}$$

$$W = \frac{M_v\ p_v}{M_a\ p_a}$$

where

M_v = 18.016

M_a = 28.96

$p_a = p_{total} - p_v$

$$= 14.696 - p_v$$

thus,

$$W = .622 \frac{p_v}{14.696 - p_v} \tag{16}$$

A first law analysis can now be obtained by the solution of Eq. (14) for various values of MA, MCW, T1, T2, TW1, and WC, where WC is the amount of water condensed.

COMPUTER PROGRAMS

The first law equation was programmed on the 7090 using the MAD language. It was first solved directly in a manner that provided a measure of its workability and flexibility. For given inlet temperatures and air flow rates, the computer calculated the cooling water flow rate required for particular exit temperatures.

A second and more sophisticated program providing more desirable conditions was then written. For various air and cooling water flow rates and continually increasing inlet temperatures, the computer calculated the corresponding exit temperatures and the amount of vapor condensed. The program format provided the output data in tabular form for easier reading. Because of the inherent characteristics of the equations involved, a trial and error procedure was required (see Flow Diagram).

As an embellishment to the project, a plot of the output data using the digital plotting system (Calcomp 780/763) was made. Using essentially the same main program, the data calculated was stored in a continuous linear array. After each graph was specified, a portion of the array was plotted (see program and plot).

DISCUSSION OF RESULTS

A brief look at the Calcomp plot makes apparent the unique characteristics of a spray condenser as compared with a conventional heat exchanger where no phase change occurs. At high inlet temperatures, the difference between the inlet and outlet temperature becomes extremely small. The heat transferred to the cooling water, in this case, is due almost entirely to that of the latent heat of condensation which results in very little temperature change of the air vapor mixture. The reason for the occurance of this at higher

FLOW DIAGRAM

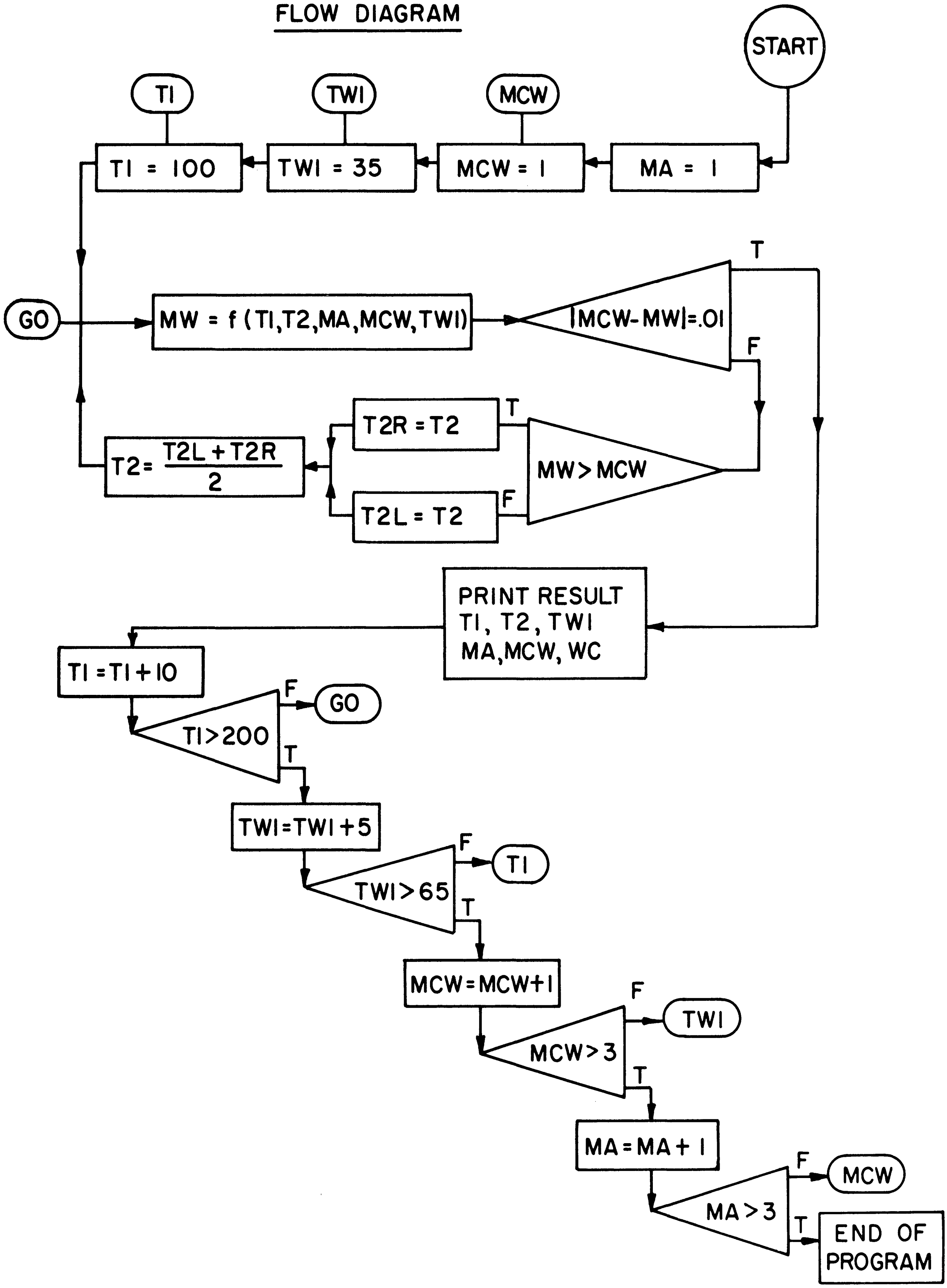

COMPUTER PROGRAM

```
            INTEGER I,J
            DIMENSION T1(882),T2(882)
            I=1
            THROUGH NEXT, FOR MCW=1.,1.,MCW.G.3.
            THROUGH NEXT, FOR MA=1.,1.,MA.G.3.
            THROUGH NEXT, FOR TW1=35.,5.,TW1.G.65.
            THROUGH NEXT, FOR T1=70.,10.,T1.G.200.
            T2L=T1
            T2R=TW1
TEMP        T2=(T2L+T2R)/2
            MW=MA*(-.241*(T2-T1)-W.(T2)*(.407*(T2+460)+877.6)
          1 +W.(T1)*(.407*(T1+460)+877.6)
          1 -(W.(T1)-W.(T2))*((T2+460)-492.52))/(T2-TW1)
            DELMW=.ABS.(MW-MCW)
            WHENEVER DELMW.LE..01
                TRANSFER TO ALPHA
            OR WHENEVER MW.G.MCW
                T2R=T2
            OTHERWISE
                T2L=T2
            END OF CONDITIONAL
            TRANSFER TO TEMP
ALPHA       T1(I)=T1
            T2(I)=T2
NEXT        I=I+1
            PLTXMX.(35.)
            PSCALE.(6.0,1.0,XMIN,DX,T2(1),98,1)
            PSCALE.(6.0,1.0,YMIN,DY,T1(1),98,1)
            PAXIS.(2.0,20.0,$T2$,-2,6.0,0.0,XMIN,DX,1.0)
            PAXIS.(2.0,20.0,$T1$,2,6.0,90.0,YMIN,DY,1.0)
            PLTOFS.(XMIN,DX,YMIN,DY,2.0,20.0)
            THROUGH PLOT1, FOR J=1.0,14.,J.G.98.
PLOT1       PLINE.(T2(J),T1(J),14,1,0,0,1)
            PSYMB.(4.0,26.0,0.2,P1,0.0,11)

            PSCALE.(6.0,1.0,XMIN,DX,T2(99),98,1)
            PSCALE.(6.0,1.0,YMIN,DY,T1(99),98,1)
            PAXIS.(10.0,20.0,$T2$,-2,6.0,0.0,XMIN,DX,1.0)
            PAXIS.(10.0,20.0,$T1$,2,6.0,90.0,YMIN,DY,1.0)
            PLTOFS.(XMIN,DX,YMIN,DY,10.0,20.0)
            THROUGH PLOT2, FOR J=99.,14.,J.G.196.
PLOT2       PLINE.(T2(J),T1(J),14,1,0,0,1)
            PSYMB.(12.0,26.0,0.2,P2,0.0,11)

            PSCALE.(6.0,1.0,XMIN,DX,T2(197),98,1)
            PSCALE.(6.0,1.0,YMIN,DY,T1(197),98,1)
            PAXIS.(18.0,20.0,$T2$,-2,6.0,0.0,XMIN,DX,1.0)
            PAXIS.(18.0,20.0,$T1$,2,6.0,90.0,YMIN,DY,1.0)
            PLTOFS.(XMIN,DX,YMIN,DY,18.0,20.0)
            THROUGH PLOT3, FOR J=197.,14.,J.G.294.
PLOT3       PLINE.(T2(J),T1(J),14,1,0,0,1)
            PSYMB.(20.0,26.0,0.2,P3,0.0,11)
```

```
        PSCALE.(6.0,1.0,XMIN,DX,T2(295),98,1)
        PSCALE.(6.0,1.0,YMIN,DY,T1(295),98,1)
        PAXIS.(2.0,11.0,$T2$,-2,6.0,0.0,XMIN,DX,1.0)
        PAXIS.(2.0,11.0,$T1$,2,6.0,90.0,YMIN,DY,1.0)
        PLTOFS.(XMIN,DX,YMIN,DY,2.0,11.0)
        THROUGH PLOT4, FOR J=295.,14,J.G.392
PLOT4   PLINE.(T2(J),T1(J),14,1,0,0,1)
        PSYMB.(4.0,17.0,0.2,P4,0.0,11)

        PSCALE.(6.0,1.0,XMIN,DX,T2(393.),98,1)
        PSCALE.(6.0,1.0,YMIN,DY,T1(393.),98,1)
        PAXIS.(10.0,11.0,$T2$,-2,6.0,0.0,XMIN,DX,1.0)
        PAXIS.(10.0,11.0,$T1$,2,6.0,90.0,YMIN,DY,1.0)
        PLTOFS.(XMIN,DX,YMIN,DY,10.0,11.0)
        THROUGH PLOT5, FOR J=393.,14.,J.G.490.
PLOT5   PLINE.(T2(J),T1(J),14,1,0,0,1)
        PSYMB.(12.0,17.0,0.2,P5,0.0,11)

        PSCALE.(6.0,1.0,XMIN,DX,T2(491.),98,1)
        PSCALE.(6.0,1.0,YMIN,DY,T1(491),98,1)
        PAXIS.(18.0,11.0,$T2$,-2,6.0,0.0,XMIN,DX,1.0)
        PAXIS.(18.0,11.0,$T1$,2,6.0,90.0,YMIN,DY,1.0)
        PLTOFS.(XMIN,DX,YMIN,DY,18.0,11.0)
        THROUGH PLOT6, FOR J=491.,14.,J.G.588.
PLOT6   PLINE.(T2(J),T1(J),14,1,0,0,1)
        PSYMB.(20.0,17.0,0.2,P6,0.0,11)

        PSCALE.(6.0,1.0,XMIN,DX,T2(589.),98,1)
        PSCALE.(6.0,1.0,YMIN,DY,T1(589.),98,1)
        PAXIS.(2.0,2.0,$T2$,-2,6.0,0.0,XMIN,DX,1.0)
        PAXIS.(2.0,2.0,$T1$,2,6.0,90.0,YMIN,DY,1.0)
        PLTOFS.(XMIN,DX,YMIN,DY,2.0,2.0)
        THROUGH PLOT7, FOR J=589.,14,J.G.686
PLOT7   PLINE.(T2(J),T1(J),14,1,0,0,1)
        PSYMB.(4.0,8.0,0.2,P7,0.0,11)

        PSCALE.(6.0,1.0,XMIN,DX,T2(687.),98,1)
        PSCALE.(6.0,1.0,YMIN,DY,T1(687.),98,1)
        PAXIS.(10.0,2.0,$T2$,-2,6.0,0.0,XMIN,DX,1.0)
        PAXIS.(10.0,2.0,$T1$,2,6.0,90.0,YMIN,DY,1.0)
        PLTOFS.(XMIN,DX,YMIN,DY,10.0,2.0)
        THROUGH PLOT8, FOR J=687,14,J.G.784
PLOT8   PLINE.(T2(J),T1(J),14,1,0,0,1)
        PSYMB.(12.0,8.0,0.2,P8,0.0,11)

        PSCALE.(6.0,1.0,XMIN,DX,T2(785.),98,1)
        PSCALE.(6.0,1.0,YMIN,DY,T1(785.),98,1)
        PAXIS.(18.0,2.0,$T2$,-2,6.0,0.0,XMIN,DX,1.0)
        PAXIS.(18.0,2.0,$T1$,2,6.0,90.0,YMIN,DY,1.0)
        PLTOFS.(XMIN,DX,YMIN,DY,18.0,2.0)
        THROUGH PLOT9, FOR J=785,14,J.G.882
PLOT9   PLINE.(T2(J),T1(J),14,1,0,0,1)
        PSYMB.(20.0,8.0,0.2,P9,0.0,11)

        PSYMB.(5.0,28.0,0.4,HEAD,0.0,47)
        PSYMB.(26.0,18.0,0.2,C1,0.0,21)
        PSYMB.(26.0,17.6,0.2,C2,0.0,22)
        PSYMB.(26.0,17.2,0.2,CW1,0.0,30)
        PSYMB.(26.0,16.8,0.2,CA,0.0,30)
        PSYMB.(26.0,16.4,0.2,CCW,0.0,37)
```

```
PSYMB.(26.0,15.4,0.2,MA1,0.0,44)
PSYMB.(26.0,15.0,0.2,MA2,0.0,44)
PSYMB.(26.0,14.6,0.2,MA3,0.0,44)
PSYMB.(26.0,14.0,0.2,MCW1,0.0,21)
PSYMB.(26.0,13.6,0.2,MCW2,0.0,21)
PSYMB.(26.0,13.2,0.2,MCW3,0.0,21)
PSYMB.(27.0,10.0,0.2,NOTE1,0.0,31)
PSYMB.(27.0,9.6,0.2,NOTE2,0.0,29)
PLTEND.
VECTOR VALUES P1=$MA=1   MCW=1$
VECTOR VALUES P2=$MA=2   MCW=1$
VECTOR VALUES P3=$MA=3   MCW=1$
VECTOR VALUES P4=$MA=1   MCW=2$
VECTOR VALUES P5=$MA=2   MCW=2$
VECTOR VALUES P6=$MA=3   MCW=2$
VECTOR VALUES P7=$MA=1   MCW=3$
VECTOR VALUES P8=$MA=2   MCW=3$
VECTOR VALUES P9=$MA=3   MCW=3$
VECTOR VALUES HEAD=$CONDENSATION RESULTS FOR EQUILIBRIUM CONDITIONS$
VECTOR VALUES C1=$T1=INLET TEMP (DEG F)$
VECTOR VALUES C2=$T2=OUTLET TEMP (DEG F)$
VECTOR VALUES CW1=$TW1=COOLING WATER TEMP (DEG F)$
VECTOR VALUES CA=$MA=DRY AIR FLOW RATE (LBS/MIN)$
VECTOR VALUES CCW=$MCW=COOLING WATER FLOW RATE (LBS/MIN)$
VECTOR VALUES MA1=$MA=1 LBS DRY AIR/MIN=18 CFM SAT AIR STD COND$
VECTOR VALUES MA2=$MA=2                 =36 CFM                 $
VECTOR VALUES MA3=$MA=3                 =54 CFM                 $
VECTOR VALUES MCW1=$MCW=1 LBS/MIN=.12 GPM$
VECTOR VALUES MCW2=$MCW=2        =.24 GPM$
VECTOR VALUES MCW3=$MCW=3        =.36 GPM$
VECTOR VALUES NOTE1=$NOTE  EACH PLOT CONTAINS TW1=35$
VECTOR VALUES NOTE2=$THROUGH TW1=65 IN 5 DEG STEPS$
END OF PROGRAM


EXTERNAL FUNCTION (T)
REFERENCES ON
ENTRY TO W.
TC=5.*(T-32.)/9.+273.16
X=647.27-TC
E=X/TC*(3.244+5.868E-3*X+1.17E-8*X.P.3)/(1+2.188E-3*X)
P=218.2/10.P.E
PV=14.696*P
W=.622*(PV/(14.696-PV))
FUNCTION RETURN W
END OF FUNCTION
```

CONDENSATION RESULTS FOR EQUILIBRIUM CONDITIONS

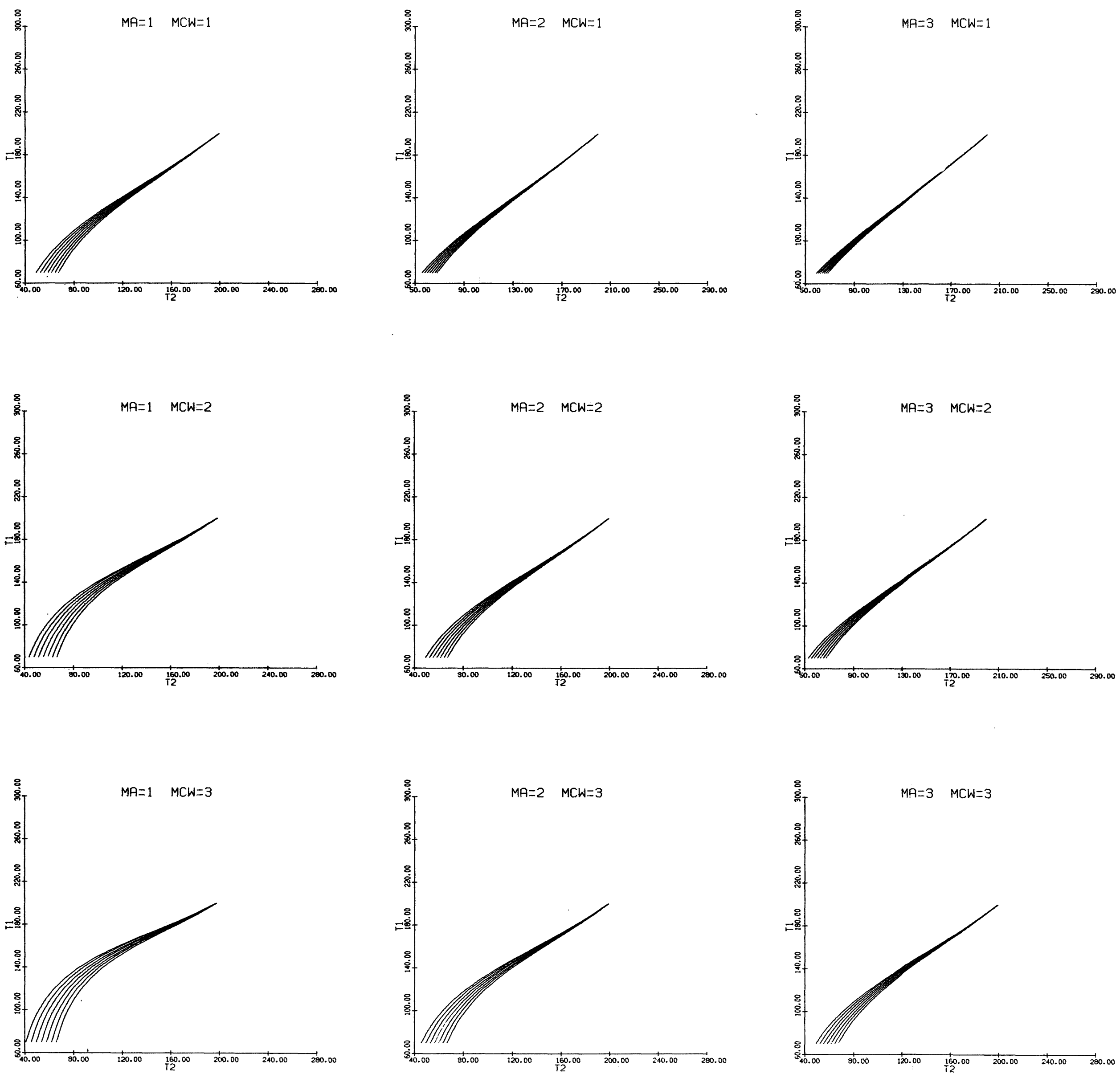

T1=INLET TEMP (DEG F)
T2=OUTLET TEMP (DEG F)
TW1=COOLING WATER TEMP (DEG F)
MA=DRY AIR FLOW RATE (LBS/MIN)
MCW=COOLING WATER FLOW RATE (LBS/MIN)

MA=1 LBS DRY AIR/MIN=18 CFM SAT AIR STD COND
MA=2 =36 CFM
MA=3 =54 CFM

MCW=1 LBS/MIN=.12 GPM
MCW=2 =.24 GPM
MCW=3 =.36 GPM

NOTE EACH PLOT CONTAINS TW1=35
THROUGH TW1=65 IN 5 DEG STEPS

temperatures is that the humidity ratio increases at a tremendous rate. That is, the vapor pressure of water is very high and results in a large amount of mass transfer. The relation between the humidity ratio and temperature is not a linear one, as can be seen by Figure 1. The data were calculated by computer using empirical equations since psychrometric charts are not available for temperatures near 200°F. The equation for the humidity ratio, included in the graph, shows that, as the temperature approaches that of the boiling point of water, the humidity ratio approaches infinity. It must be noted, however, that the actual inlet air conditions of the spray condenser may not be near saturation at high temperatures since a large amount of heat and mass transfer must occur.

The effects of air and cooling water flow rates can be seen by observing the variation in the graphs from left to right for air and from top to bottom for cooling water.

The effects of cooling water temperature, TW1, are hard to ascertain from the Calcomp plot because of latent heat of condensation involved. A plot of inlet temperature versus water vapor condensed (Figure 2) is more effective. At 180°F the water vapor condensed increases by 24% as the cooling water temperature varies from 65°F to 35°F.

The amount of heat and mass transferred during the condensation process is illustrated in the flow diagram (Figure 3). The latent heat of condensation is indeed predominant in comparison with the "sensible" heat transfer.

REMARKS ON CONDENSER DESIGN

Spray condensers are used in air conditioning and in the chemical industry. However, their design procedures are not generally based on theoretical considerations, since there is no definite surface area for heat exchange and no easily determined heat and mass transfer coefficients. Therefore, a rigorous theoretical approach cannot be expected. It is felt that the time-dependent equations of heat transfer and mass transfer could supplement a particular design if the theoretical and experimental approaches were integrated. The first law analysis is, of course, not time dependent and thus deviates from the real system. It does, however, provide much insight into the condensation process and establishes boundaries within which the real system must operate.

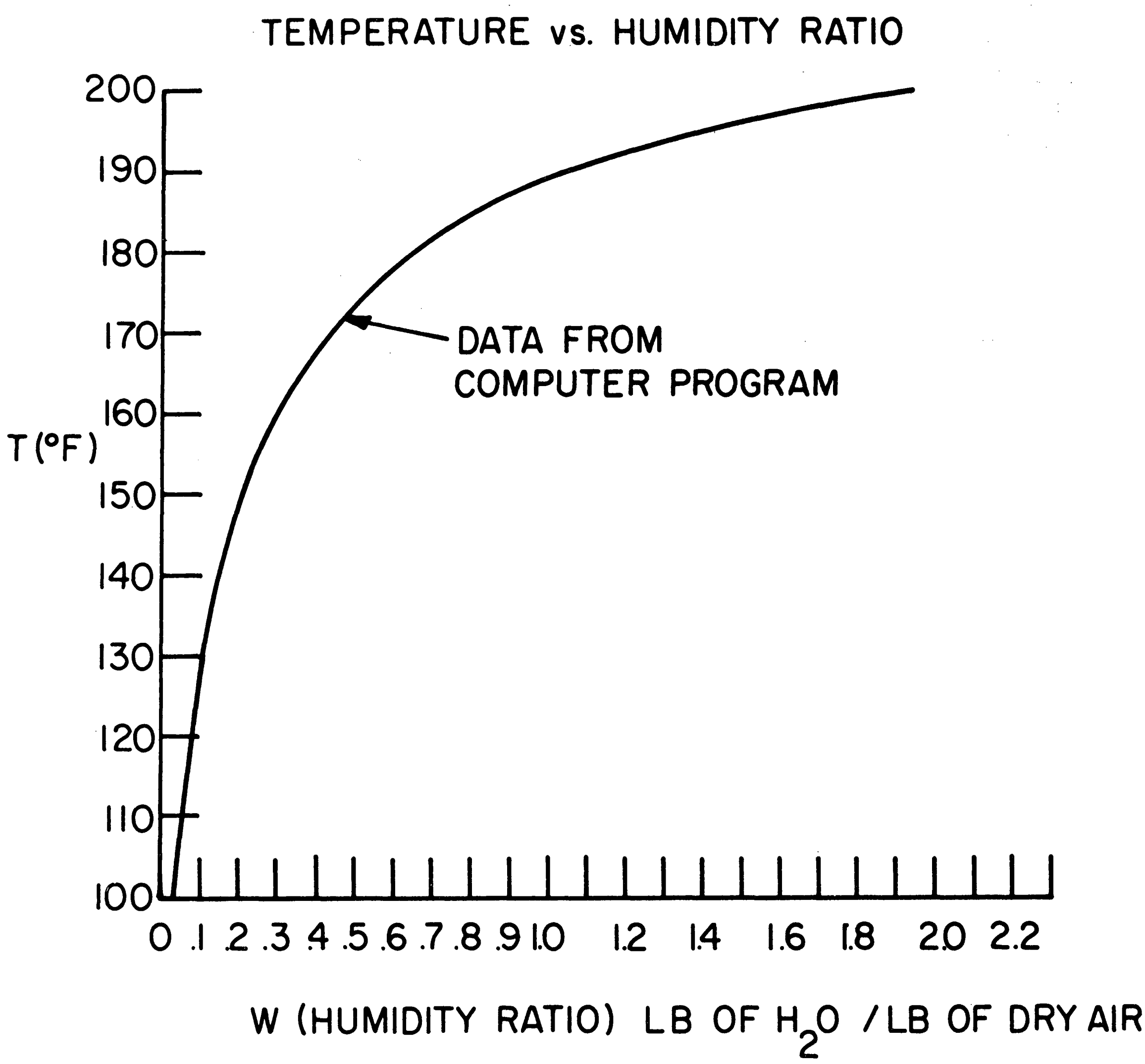

$$W = .622 \frac{p_v}{p_{total} - p_v} \qquad p_{total} - p_v = p_{air}$$

Figure 1. Shows that the humidity ratio goes to infinity when the vapor pressure approaches the ambient pressure (i.e., near boiling).

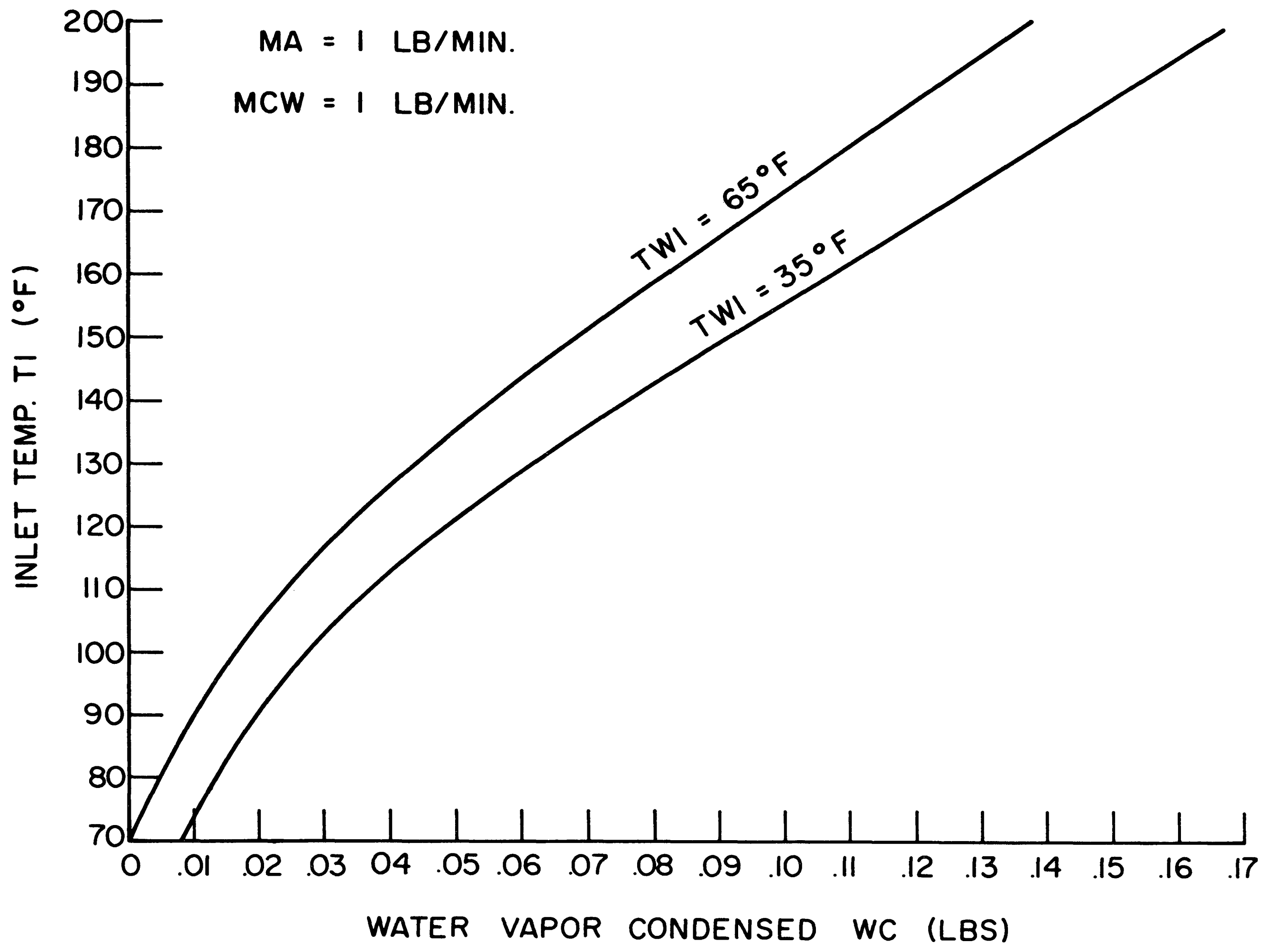

Figure 2. T1 vs. WC.

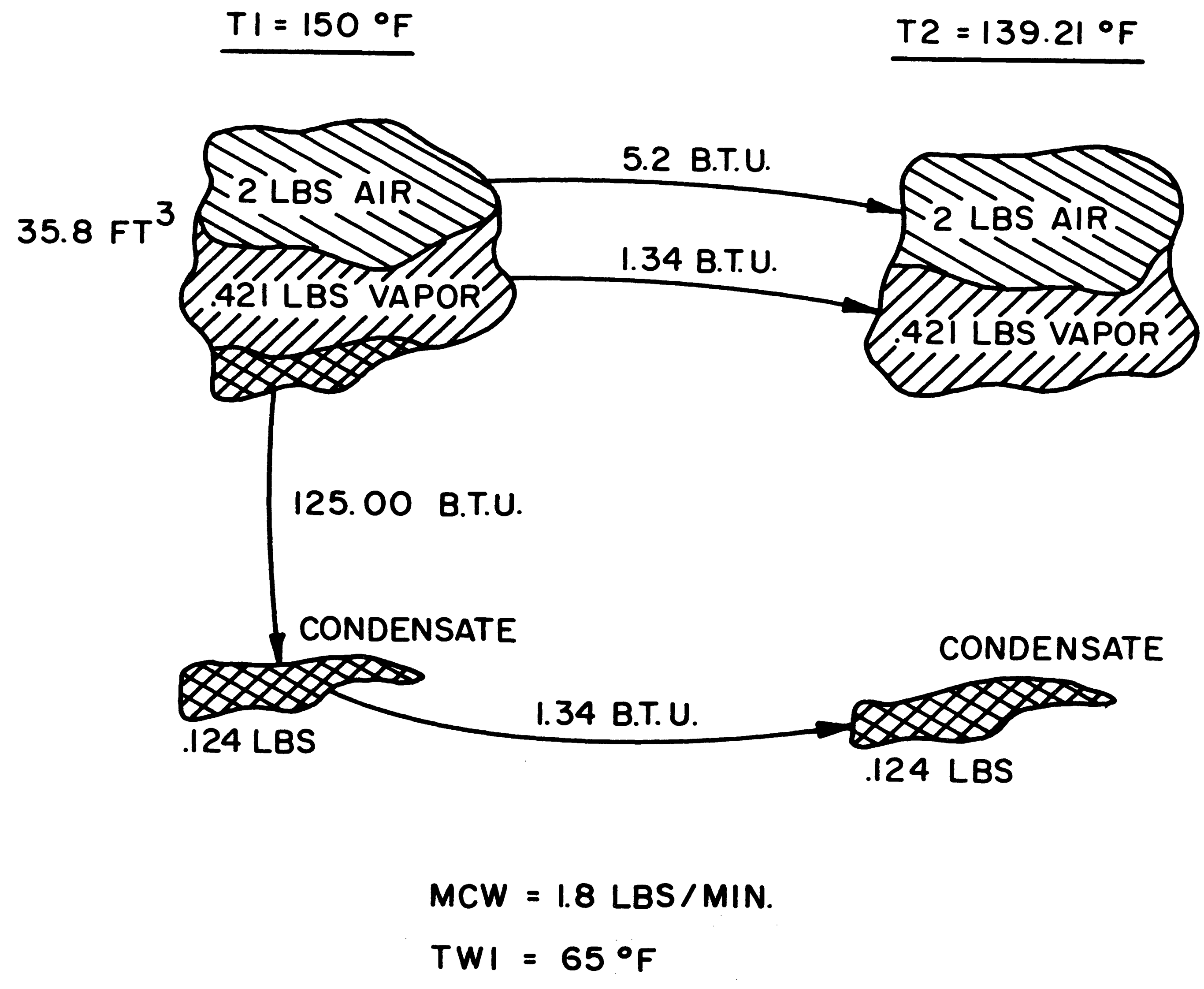

Figure 3. Heat and mass transfer during condensation.

NOZZLE MATERIAL CONSIDERATIONS

A talk with Professor Ken C. Ludema of The University of Michigan about material and wear considerations of the extraction nozzle and cylinder provided the following information and suggestions.

The combination of Delrin or Nylon rubbing on a stainless steel drum is good. Both have good wear-resistant qualities for a plastic, and their temperature limitation is high (500°F). Possibly, a better nozzle material is Delrin A.F. It has 22% by wt. Teflon fibers which would coat the stainless steel screen during operation. Another compatible combination is a Nylon nozzle rubbing on a Teflon coated screen.

REFERENCES

1. Fronczak, E., The University of Michigan Digital Plotting System, 1965.

2. Kreith, Principles of Heat Transfer, Chapter 9, Massachusetts Institute of Technology Press, 1964.

3. Keenan, J. H., and F. G. Keyes, Thermodynamic Properties of Steam, Wiley, New York, 1965.

4. Van Wylen, G. J., Thermodynamics, Wiley, New York, March 1963.

BIBLIOGRAPHY

Chemical Engineering, "Direct Contact Heat Transfer," p. 184, August 1963.

Fronczak, E., *The University of Michigan Digital Plotting System*, 1965.

Griffith, P., *Development in Heat Transfer*, Chapter 9, Massachusetts Institute of Technology Press, 1964.

Keenan, J. H., and F. G. Keyes, *Thermodynamic Properties of Steam*, Wiley, New York, January 1965.

Kreith, *Principles of Heat Transfer*, Chapter 13, International Textbook, January 1964.

McAdams, W. H., *Heat Transmission*, Chapter 9, McGraw-Hill, New York, 1933.

Organick, E. I., *A MAD Primer*, University of Houston, 1964.

Refrigeration Engineering, "Conditioning of Hot Humid Air," November 1948, p. 417.

Schock, A., *Industrial Heat Transfer*, Chapter 3, Wiley, New York, 1933.

Streeter, V. L., *Fluid Mechanics*, McGraw-Hill, New York, 1962.

Tek, M. R., "Mechanic of Multiphase Flow," manuscript and notes for CM 522, University of Michigan, owned by Kenneth Volkers.

University of Michigan Algorithm Decoder, University of Michigan, March 1965.

Van Wylen, G. J., *Thermodynamics*, Wiley, New York, March 1963.

DESIGN CHARACTERISTICS OF AIR-WATER SEPARATORS FOR HOME LAUNDRY APPLIANCES

Douglas H. Lane

NOMENCLATURE

Symbol	Dimensions	
a	in.^{2}	inlet area perpendicular to gas flow
A	in.^{2}	inside surface area exposed to spinning gas
D_I	in.	inlet diameter
D_C	in.	cyclone diameter
D_E	in.	exit diameter
g	ft/sec^2	gravitational acceleration
G	----	friction factor
K_L	----	head loss coefficient
P	lb/in.^{2}	pressure inside separator
ΔP	in. of water	pressure drop across separator
Q	ft^3/min	volumetric flow rate
R	in.	radius
R_1	in.	mean inlet radius of vortex
R_2	in.	effective exit radius of vortex = $R_E/2$
R_I	in.	radius of circle to which center line of inlet is tangent
R_E	in.	exit duct radius
T	°F	average of inlet and outlet temperature
U_1	ft/sec	spinning speed at mean inlet radius R_1
U_2	ft/sec	spinning speed
V_I	ft/sec	inlet air velocity

NOMENCLATURE (Continued)

Symbol	Dimensions	
V_E	ft/sec	exit duct air velocity
φ	----	velocity ratio U_1/V_I
ρ	lb/ft^3	separator air density

DEFINITION OF THE PROBLEM

The problem is defined as the portion of the extraction and dry cycle of the experimental combination washer and dryer which includes all parts from the extraction nozzle to and including the separator. The object of the study is to mathematically define the performance of the extraction and dry cycle to determine an optimum design by the use of a digital computer.

PRELIMINARY LIBRARY SEARCH

A preliminary library search was conducted on vacuum extraction drying. The literature on this subject dealt with textile applications in which the motion of the wet fibers could be carefully controlled. No direct conclusions could be drawn from this literature for application to the extraction cycle. References (1), (2), and (5) were published in Textile Recorder, a periodical which was not available for review. These articles might be of some benefit in the area of vacuum extraction drying.

AREA OF CONCENTRATED STUDY: THE SEPARATOR

The separator was selected as the area of concentrated study. The function of the separator is to remove liquid water and lint without obstructing the extraction and dry cycle. Overall efficiency is the most important separator design consideration. By overall efficiency is meant consideration of the entire extraction and dry cycle performance, rather than consideration of the separator by itself. A less-than-optimum separator design may give optimum extraction and dry cycle performance. Specific areas to be optimized are separation time, power, cost, weight, strength, size, space, geometry, and maintenance.

INVESTIGATION OF TYPES OF SEPARATORS

Different types of separators were investigated to determine their applicability. The cyclone (centrifugal) separator was selected for detailed study because of its relatively constant efficiency over a wide range of operating conditions, small pressure drop, simplicity, size, and cost.

The cyclone scrubber was rejected because a pump would be required to produce a condensing water spray under pressure of 60-200 psi inside the separator and because of the possibility of reentrainment (Refs. 4,5). It is more efficient and economical to introduce the condensing water upstream under no pressure and thereby eliminate the need for a pump.

The electric precipitator was rejected because of high cost (transformer and rectifier), safety (30,000 to 100,000v), and maintenance (Ref. 6).

Cloth filters were rejected because of their large size and tendency to clog, causing a large pressure drop and requiring maintenance (Ref. 5).

Power driven separators were rejected, in general, because of the need for a pump or motor.

THEORY OF SEPARATION IN A CYCLONE SEPARATOR

In a cyclone separator, the fluid enters the chamber tangentially at one or more locations and leaves through a central opening. The water droplets, by virtue of their inertia, tend to move toward the outside separator wall and run down the cylinder wall. The particle acceleration is in the range of 5g in very large-diameter and low-resistance separators, and 2500g in very small-diameter and high-resistance units (Ref. 7). In addition to the tangential flow pattern, a double vortex is present where the gas spirals down at the outside and up at the inside. The tangential flow direction is the same for the descending and ascending vortexes. These velocities are small but may tend to move reentrained water.

Any inefficiency of water separation is due to reentrainment or wall creep of liquid film after the spray has been deposited on the cyclone wall. The liquid film is carried across the cyclone roof to the gas outlet duct by double-eddy action. The film then runs down the outside of this duct and is picked up by the air as it enters the exit duct (Ref. 7). This phenomenon was not observed in a clear separator while operating in an experimental washer and dryer. The double-eddy action can be minimized by providing a concentric cylindrical shield around the gas outlet duct or a conical skirt fastened to the outside at some distance above the mouth of the outlet duct. This avoids reentrainment by providing a drip point before the liquid is exposed to the outlet gas stream.

The cyclone separator will operate equally well on the suction or pressure side of a fan and in a vertical or horizontal position when separating dust. Gravitational effects on the condensing water may prohibit the operation of the separator with the exit duct axis in a horizontal direction. A slight air leak will reduce efficiencies. Generally, cone and disk baffles, helical guide vanes, and straightening vanes inside the separator have a detrimental effect. An inlet vane will reduce pressure drop, but will reduce collection efficiency even more by increasing reentrainment. Direct impingement of the inlet gas stream on the reentrainment shield should be avoided in water separation by increasing the cyclone diameter (Ref. 8). The exit duct should extend inside the separator about 1-1/2 time the duct diameter for maximum efficiency for dust separation (Ref. 9). This may not be true for water separation. The inlet velocity should be less than 150 ft/sec for water separation (Refs. 7,8). A cyclone diameter of 2-3 inches is a practical minimum (Ref. 8). The optimum ratio of cyclone diameter to exit diameter is about 2-3 (Ref. 8). Increasing the length of the body provides a longer time for separation and prevents water from being picked up by the air leaving the exit duct (Ref. 8). The height of the separator should be at least $6D_E$ and preferably $(8\text{-}12)D_E$ (Ref. 8).

The theories of separation and particle dynamics were studied to gain an understanding of the process of separation (Ref. 7). Most of the work on cyclone separators has been done with separation of dust from air. Information on dust separation can be applied to liquid water separation. In addition, water tends to agglomerate and reentrain. Particle size is an important variable in dust separation efficiency. Cyclone separators will do a good job of collecting water droplets of 5 microns diameter (4×10^{-5} in) or larger (Ref. 8). The size of atmospheric fog droplets is 2-15 microns. It is apparent from visual observations that the water droplets are larger than fog droplets. Therefore, it can be concluded that separation efficiency is not a major variable in the design of the separator for use in the extraction and dry cycle.

It has been assumed that pressure drop across the separator is the major design consideration, because collection efficiency should be satisfactory with any reasonable cyclone design. The power required to produce the air flow is directly proportional to the pressure drop in the entire extraction and dry cycle. The power required for the air flow across the separator will be minimum if the pressure drop across the separator is minimum.

PRESSURE DROP IN CYCLONE SEPARATORS

C. J. Starimand has derived an equation for the pressure drop in cyclone separators (Ref. 10). Pressure drops due to the inlet kinetic head, centrifugal head in the vortex, and the exit duct losses are considered separately.

The inlet kinetic head loss is

$$\Delta P_1 = \frac{\rho \, V_I^{\,2}}{2 \, g} \tag{1}$$

The centrifugal vortex loss has been shown to be

$$\Delta P_2 = 2 \left[\frac{\rho \, U_2^2}{2g} - \frac{\rho \, U_1^2}{2g} \right]$$

For the exit duct loss, it has been assumed that the spinning fluid at the center of the cyclone has no velocity component along the center of the axis of the exit pipe. The energy loss is the energy supplied to accelerate the air in the direction of the exit duct. The exit duct loss has been experimentally determined to be

$$\Delta P_3 = 2\left(\frac{\rho V_E^2}{2g}\right) \tag{3}$$

Attempts to recover any kinetic head at the exit duct were unsuccessful. Summing Eqs. (1), (2), and (3)

$$\Delta P = \Delta P_1 + \Delta P_2 + \Delta P_3 = \frac{\rho V_I^2}{2g} + 2\left(\frac{\rho U_2^2}{2g} - \frac{\rho U_1^2}{2g}\right) + 2\left(\frac{\rho V_E^2}{2g}\right) \tag{4}$$

Vortex spinning speed can be greater, equal, or less than the inlet velocity depending on the geometric proportions of the separator. Experimentally,

$$U_R^2 \;\; R = C_1 \qquad \text{for } R > \frac{R_E}{2}$$

$$U_R \;\; R = C_2 \qquad \text{for } R < \frac{R_E}{2}$$

By momentum considerations, Stairmand has shown that the ratio of vortex spinning velocity to inlet velocity is

$$\varphi = \frac{U_1}{V_I} = \frac{\sqrt{\frac{R_E}{2R_I}} + \sqrt{\frac{R_E}{2R_I} + \frac{4GA}{a}}}{\frac{2GA}{a}} \tag{5}$$

For a circular inlet duct,

$$\frac{R_E}{2R_I} = \frac{D_E}{2(D_c - D_I)} \tag{6}$$

Substituting Eq. (6) into Eq. (5)

$$\varphi = \frac{U_1}{V_I} = \frac{\sqrt{\dfrac{D_E}{2(D_c-D_I)}} \quad \sqrt{\dfrac{D_E}{2(D_c-D_I)}} \quad \dfrac{4GA}{a}}{\dfrac{2GA}{a}} \tag{7}$$

$$U_1 = \varphi V_I \tag{8}$$

$$U_2 = \varphi V_I \sqrt{\frac{R_1}{R_2}} = \varphi V_I \sqrt{\frac{2R_E}{R_I}} = \varphi V_I \sqrt{\frac{2(D_c-D_I)}{D_E}} \tag{9}$$

$$Q_E = Q_I, \text{ for } \rho = C. \tag{10}$$

This assumption is valid because the maximum temperature change across the separator is less than 10°F.

$$V_E \frac{\pi}{4} D_E^2 = V_I \frac{\pi}{4} D_I^2 \tag{11}$$

$$V_E^2 = V_I \left(\frac{D_I}{D_E}\right)^4 \tag{12}$$

Assuming the ideal gas law:

$$\rho = \frac{P}{R(T+460)} \tag{13}$$

Substituting Eqs. (12), (9), (8), and (7) into Eq. (4),

$$\Delta P = \frac{P\, V_I^2}{2gR(T+460)} \left[1 + 2\,\varphi^2 \left(\frac{2(D_c-D_I)}{D_E} - 1 \right) + 2\left(\frac{D_I}{D_E}\right)^4 \right] \tag{14}$$

USE OF THE COMPUTER

The purpose of using the computer is to try all possible diameter size combinations to determine an optimum separator design to give the lowest pressure drop for any operating condition. For design optimization, it is convenient to convert the pressure drop equation to dimensionless form in terms of diameter ratios rather than individual diameter dimensions. The three important variables that determine the performance of the separator are inlet, outlet, and cyclone diameters. The separator length and the distance the exit duct extends into the separator are of secondary importance. The friction factor is not known, but Stairmand has shown that the friction factor is about (1/200) for most operating conditions. For greater accuracy, it may be desirable to determine the friction factor for the separator material.

Converting the pressure drop equation into a dimensionless form:

$$\text{Let } K_1 = \frac{D_I}{D_E} \tag{15}$$

$$K_2 = \frac{D_c}{D_E} \tag{16}$$

A—inside surface area of cyclone exposed to spinning fluid, considering the separator top and bottom, the separator walls, and the outside of the exit duct.

$$A = 2\left(\frac{\pi}{4} D_c^2\right) + \pi L_c D_c + \pi L_E D_E \tag{17}$$

a—inlet area perpendicular to the gas flow

$$a = \frac{\pi}{4} D_I^2$$

$$G = \frac{1}{200}$$

$$\text{Let } K_3 = \frac{GA}{a} = \left(\frac{1}{200}\right) \frac{\left(\frac{\pi}{2} D_c^2 + \pi L_c D_c + \pi L_E D_E\right)}{\frac{\pi}{4} D_I^2} \tag{18}$$

$$K_3 = \left(\frac{1}{50}\right) \left[\frac{1}{2} \frac{D_c^2}{D_I^2} + L_c \frac{D_c}{D_I^2} + L_E \frac{D_E}{D_I^2}\right]$$

Let $N = \dfrac{L_c}{D_c}$, $M = \dfrac{L_E}{D_E}$

$$K_3 = \left(\frac{1}{50}\right)\left[\frac{1}{2}\,\frac{D_c^2}{D_I^2} + N\,\frac{D_c^2}{D_I^2} + M\,\frac{D_E^2}{D_I^2}\right] = \frac{1}{50}\left[\frac{\left(\frac{D_c}{D_E}\right)^2}{\left(\frac{D_I}{D_E}\right)^2}(.5 + N) + \frac{M}{\left(\frac{D_I}{D_E}\right)^2}\right] \tag{19}$$

$$K_3 = \left(\frac{K_2}{K_1}\right)^2 \frac{\left(.5 + N + \frac{M}{K_2^2}\right)}{50} \tag{20}$$

$$\text{Let } K_4 = \frac{D_E}{2(D_c - D_I)} = \frac{1}{2\left(\frac{D_c}{D_E} - \frac{D_I}{D_E}\right)} = \frac{1}{2(K_2 - K_1)} \tag{21}$$

$$\text{From (7)} \quad \varphi \; \frac{\sqrt{\dfrac{D_E}{2(D_c - D_I)}} + \sqrt{\dfrac{D_E}{2(D_c - D_I} + \dfrac{4GA}{a}}}{\dfrac{2GA}{a}} \tag{22}$$

$$\varphi = \frac{-\sqrt{K_4} + \sqrt{K_4 + 4K_3}}{2K_3} \tag{23}$$

$$\text{Let } B = 2\varphi^2 = 2\left(\frac{\sqrt{K_4} + \sqrt{K_4 + 4K_3}}{2K_3}\right)^2 = \frac{K_4 + 2K_3 - \sqrt{K_4^2 + 4K_3K_4}}{K_3^2} \tag{24}$$

Substituting Eqs. (15), (21), and (24) into Eq. (14)

$$\Delta P = \frac{PV_I^2}{2g(R)(T+460)}\left[1 + B\left(\frac{1}{K_4} - 1\right) + 2\,K_1^4\right] \tag{25}$$

with V_I - ft/sec

P - lb/in.^{2}

T - °F

ΔP - in. of water

$$\Delta P = (P)\left(144 \frac{in^2}{ft^2}\right)(V_I^2)\left(.01602 \frac{\text{in. of water}}{\frac{lb}{ft^2}}\right)\left(\frac{\text{12 in. of water}}{\text{ft. of water}}\right)$$

$$\left[1 + B\left(\frac{1}{K_4} - 1\right) + 2K_1^4\right] \qquad (26)$$

$$\Delta P = \frac{(.00808)\ P\ V_I^2}{(T+460)}\left[1 + B\left(\frac{1}{K_4} - 1\right) + 2K_1^4\right]$$

The pressure drop as it appears in Eq. (27) is the final form as used in the computer program.

COMPUTER PROGRAM

The MAD computer program on Page 83 of the Appendix can be used to determine an optimum separator design for any volumetric flow rate and a range of inlet velocities. The pressure drop is computed by using Eq. (27). Equations (15), (16), (20), (21), and (24) are used in the program for computation of intermediate values. Three iteration loops are included in the program. The first iteration loop assumes a specified inlet velocity. The other two iteration loops are used to determine the optimum combination of inlet to exit and cyclone to exit duct diameter ratios. These two iteration loops consider all possible combinations of the two different diameter ratios over a specified range of values, in specified increments, for each diameter ratio. The combination of diameter ratios for minimum pressure drop is theoretically the same for all operating flow conditions. The size of the separator is determined by the flow conditions.

Assuming a known Q, volumetric flow rate, and a known inlet velocity V_I, the inlet diameter is calculated by letting

$$V_I a = V_I \frac{\pi}{4} D_I^2 = Q \qquad (28)$$

$$D_I^2 = \frac{4}{\pi}\frac{Q}{V_I} = \frac{(4)\ Q(144\ \frac{in.^2}{ft^2})}{\pi\ V_I\ (60\ \frac{sec}{min})} = 3.06\ \frac{Q}{V_I}$$

$$D_I = 1.75\sqrt{\frac{Q}{V_I}}$$

Assuming no space limitations, it can be concluded that, for minimum pressure drop, K_1 should be as small as possible. Physically, this means the exit diameter should be as large as possible. The diameter ratios are restricted by physical rather than mathematical limitations; it may not be possible to build a separator with the optimum diameter ratios.

If certain restrictions are imposed on the separator design, the computer program can be rearranged to determine the optimum design with the restrictions taken into consideration.

A second MAD computer program on Page 84 of the Appendix can be used to calculate the analytical pressure drop of various separators for the specific operating conditions. This program can be conveniently used to calculate the pressure drop of different separators under a wide range of operating conditions.

The use of the two MAD computer programs is restricted to separator designs with a circular inlet and no reentrainment shield. The computer program can be developed to consider other types of inlet configurations. The influence of a reentrainment shield on pressure drop would have to be determined experimentally before its effect could be considered in the computer program.

EXPERIMENTAL TESTS

The operating conditions of the separator in the extraction and dry cycle differ from those of Stairmand's experiments, because water rather than dust is being separated in the extraction and known and is not considered in the pressure drop equation.

Tests were conducted on two different separators to compare the tests results with the analytical pressure drop as predicted by the pressure drop equation, and to determine the effect of water on pressure drop. Tests were conducted at four different operating conditions: 1. No heat added and no water; 2. Heat added and no water; 3. No heat added with water; 4. Heat added with water.

The separator test set-up is illustrated in Figure 1. It was necessary to add straightening vanes before the pitot tube to eliminate the spinning in the fluid in order to determine the volumetric flow rate accurately. Discrepancies due to the spinning fluid are also introduced in measuring the pressure drop across the separator. Stairmand has unsuccessfully tried to eliminate these effects, but he believes the general agreement is reasonable.

To isolate the separator from the effects of bends, contractions, and other influences, 20 inches of straight duct was added to the inlet duct and 17 inches of straight duct was added to the exit duct. Pressure taps were placed in the middle of these added ducts.

The first separator tested was an early prototype whose dimensions are shown in Figure 2. The pressure drop can be analytically determined by using the computation MAD computer program on page 84 of the Appendix.

The results of the experimental tests and the analytical determination of the pressure drop are plotted in Figure 3. The analytical results for test conditions 1 and 3 were, for all practical purposes, the same and are plotted as one line. The same reasoning applied to test conditions 2 and 4. The experimental and the analytical results of the two test conditions of 1, no heat with no water, and 2, heat with no water, correspond very well. For the two test conditions of 3, no heat with water, and 4, heat with water, the analytical results are approximately twice the experimental test results.

It can be concluded that there is good correlation between the experimental and analytical results when no water is present for this particular separator. Water markedly reduces the pressure drop across the separator.

The second separator tested was a later prototype whose dimensions are shown in Figure 4. The presence of the reentrainment shield is not considered in the pressure drop equation. By ignoring the influence of the reentrainment shield, except for its contribution to friction, the analytical results are four times the experimental results.

The next analytical attempt has been to consider the diameter of the reentrainment shield as the equivalent exit diameter, and to add an additional pressure drop term due to the contraction between the reentrainment shield and the actual exit duct.

The results of the experimental tests and the analytical determination of the pressure drop are plotted in Figure 5. The analytical results for test conditions 1 and 3 were, for all practical purposes, the same and are plotted as one line. The experimental test results are nearly the same for all four test conditions. The analytical results are nearly the same for all four test conditions. The experimental test results are in the order of 1-1/2 to 2 times as great as the analytical results.

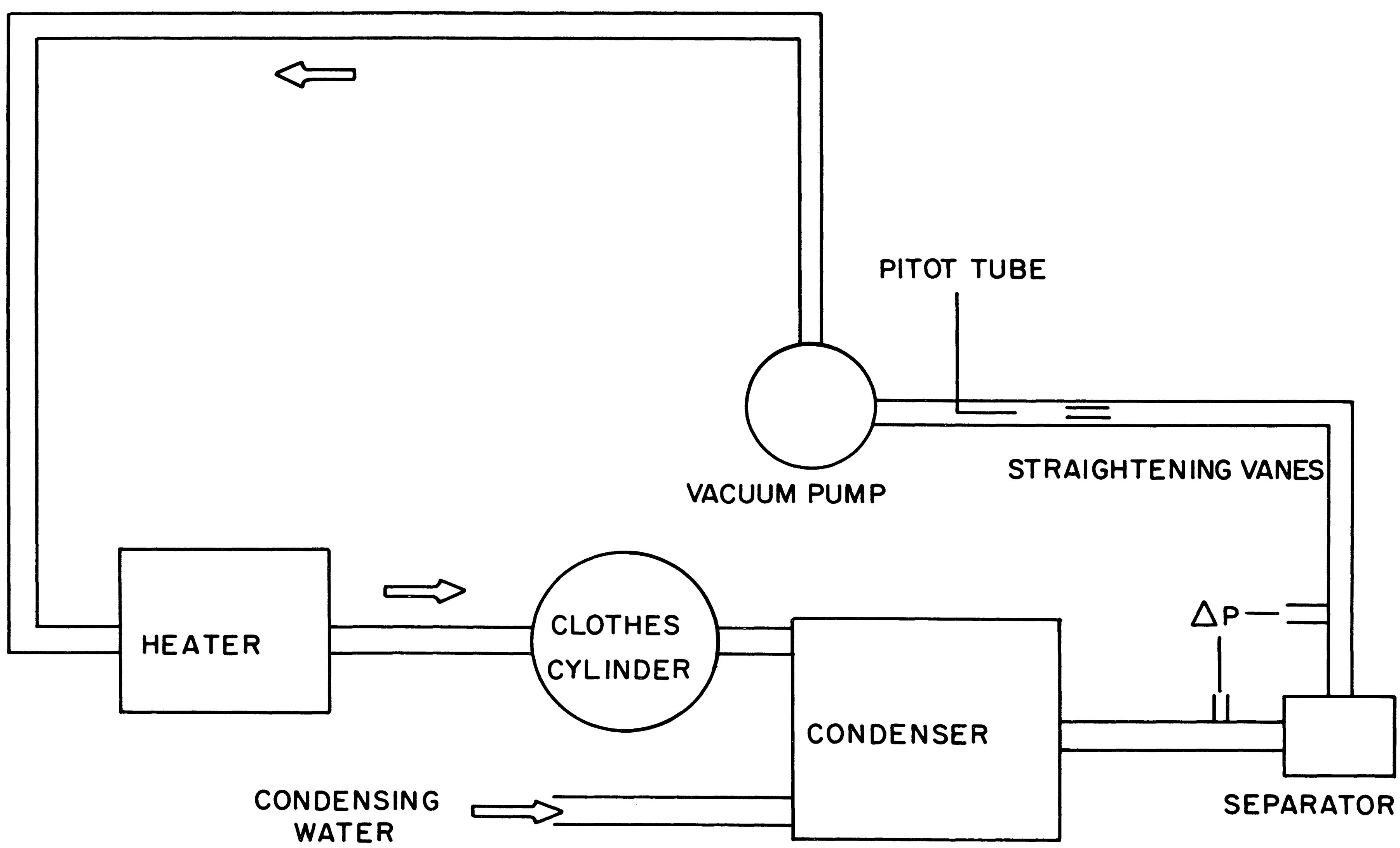

Figure 1. Test-setup

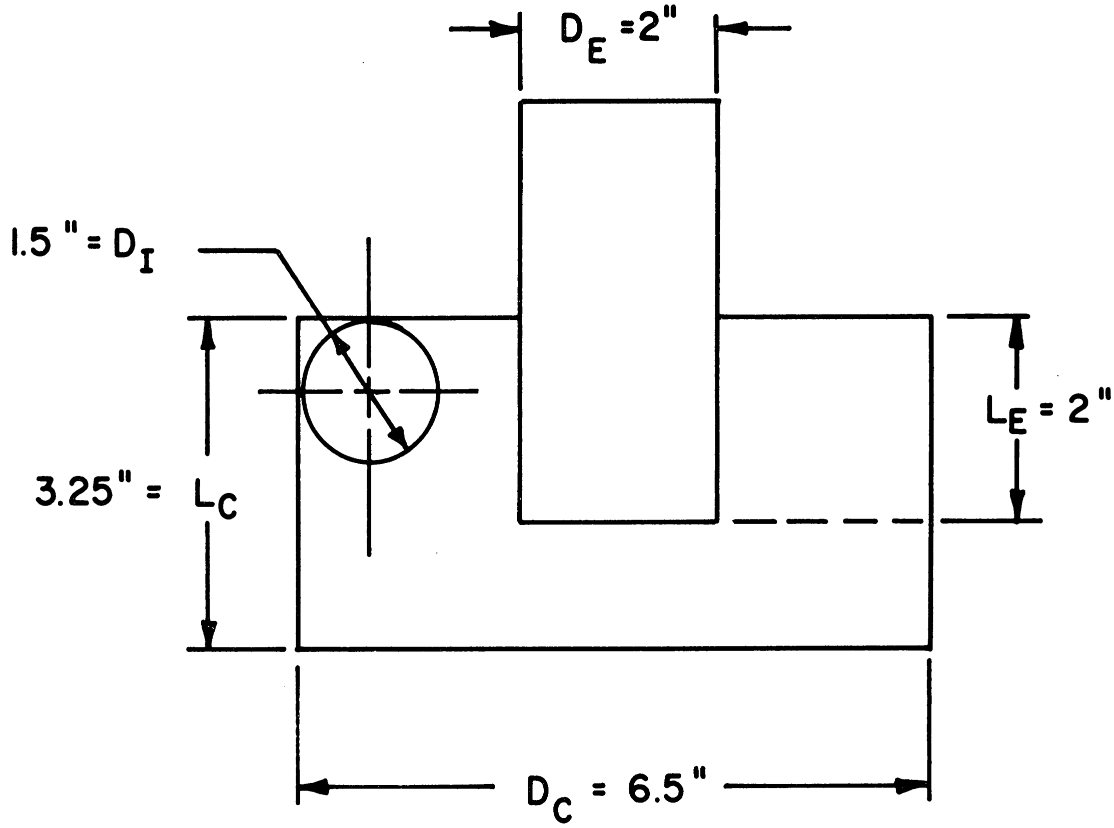

Figure 2. Clear separator.

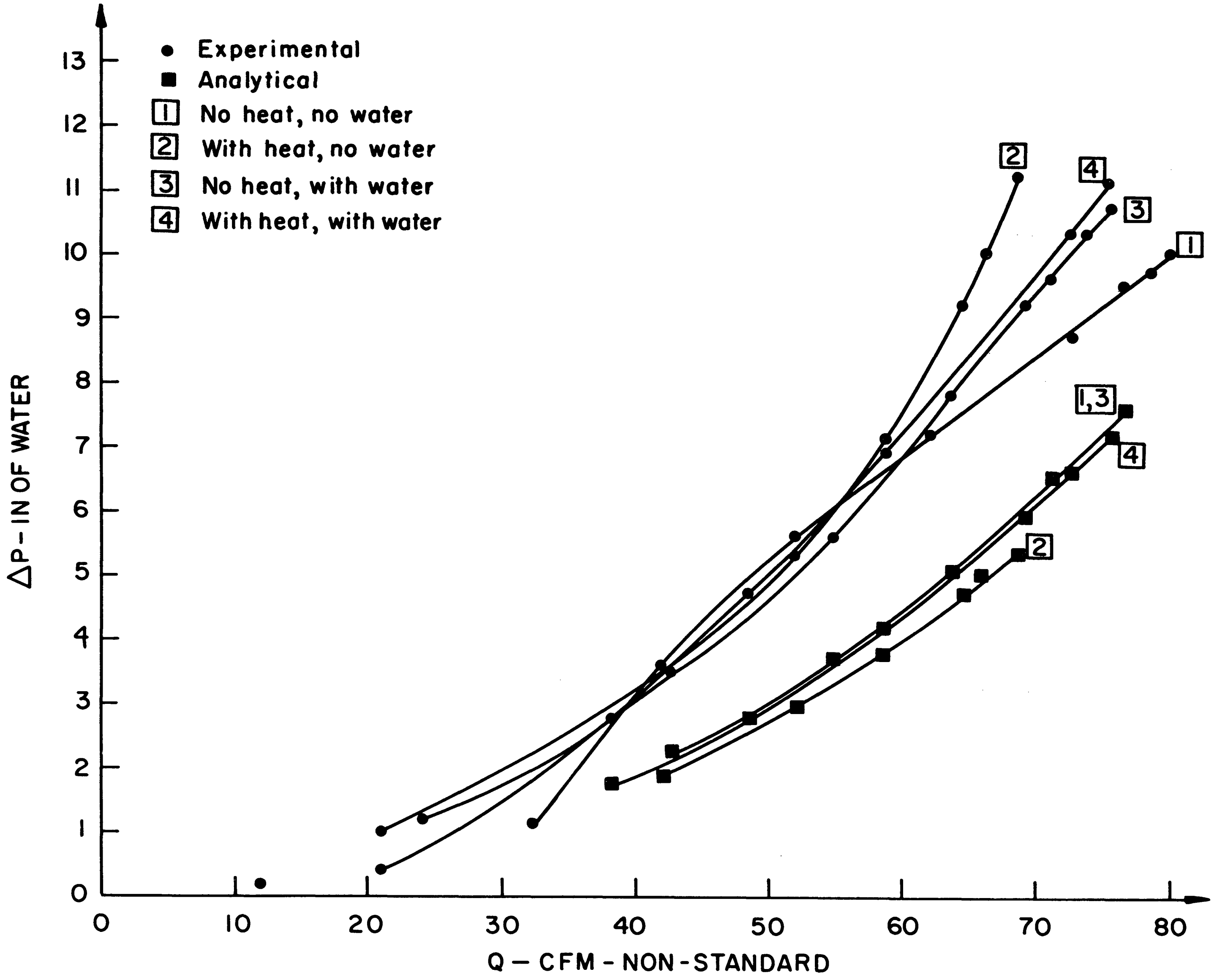

Figure 3. Pressure drop vs. volumetric flow rate (clear separator).

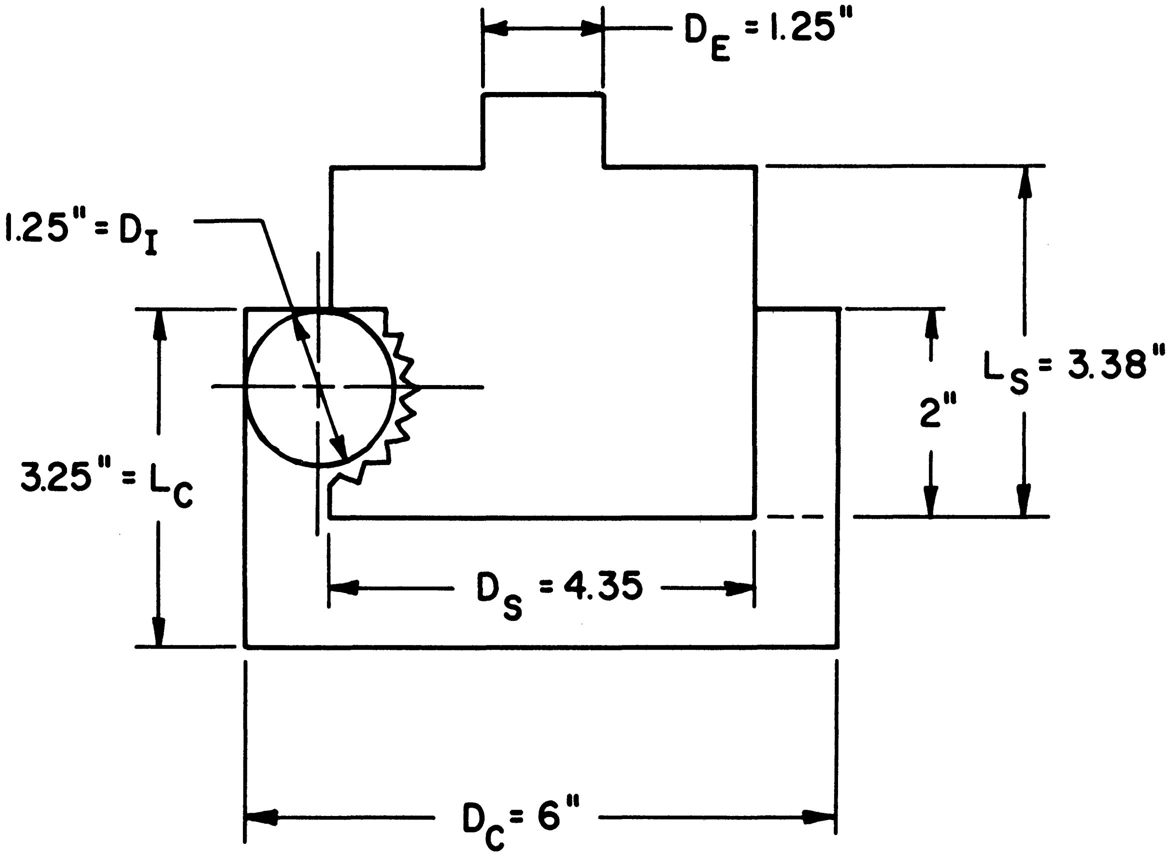

Figure 4. Black separator.

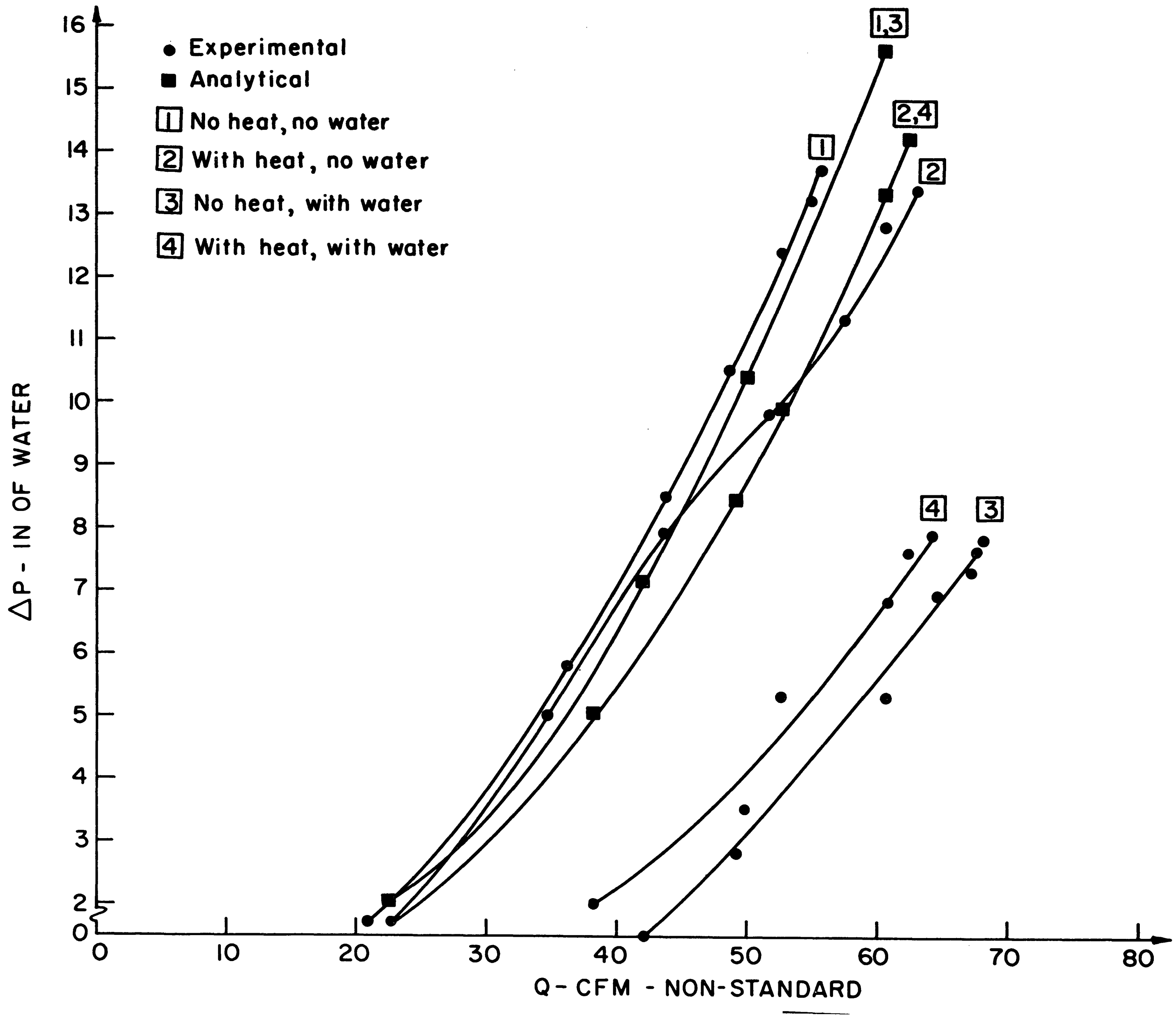

Figure 5. Pressure drop vs. volumetric flow rate (clear separator).

It can be concluded with this separator design that the separator performance is nearly the same under all four test conditions. The influence of the reentrainment shield is not known. The analytical results are better than the first analytical attempt, but the correlation with the experimental results is not strong enough to be used for design purposes.

CONCLUSIONS AND FUTURE WORK

It can be concluded from the computer results that the exit duct diameter should be as large as possible. The minimum diameter ratios are restricted by physical limitations rather than mathematical limitations. According to the pressure drop equation, all optimum separator designs are geometrically similar when pressure drop is the only consideration. This ignores any influences of the separator on the extraction and dry cycle. The influence of the separator design on the extraction and dry cycle during non-steady state conditions is not known and will be a topic of future investigation.

The results of the separator tests are inconclusive. The influence of water on pressure drop is not known. The influence of a reentrainment shield on pressure drop is not known. More tests should be run on different separator designs.

Future work will involve the building of two or three separators using present separator knowledge as a guide. The separators will be built and tested during the summer of 1966 and I will continue the work in the fall. A final report will be written on the results of these tests at the end of the fall term.

REFERENCES

1. Carpenter, A., "Drying of Hosiery Goods," Textile Recorder, LXIX, No. 805, April 1950, pp. 84-85.

2. ______, "High Efficiency Cylinder Drying Machine," Textile Recorder, LXXXI, No. 965, August 1963, pp. 68-70.

3. McMahon, G. B., and J. G. Downes, "New Open Width Suction Extractor," Textile Recorder, LXVII, No. 805, April 1950, pp. 84-85.

4. Kleinschmidt and Anthony, "Recent Development of Cyclone (Rease-Anthony) Scrubber," A.S.M.E. Transactions, LXIII, No. 349, 1941.

5. Perry, ed., "Cyclone Separators," C. E. Engineers Handbook, 1950, p. 1023.

6. Peters, "Electrical Precipitators," C. E. Engineers Handbook, 1963, pp. 20-80.

7. Perry, ed., "Cyclone Separators," C. E. Engineers Handbook, 1950, p. 1023.

8. Caplan, K. J., "All About Cyclone Collectors," Air Engineering, VI, No. 9, September 1964, pp. 28-38.

9. ter Linden, A. J., "Investigations into Cyclone Dust Collectors," Institution of Mechanical Engineers, September 1949, p. 233.

10. Stairmand, C. J., "Pressure Drop in Cyclone Separators," Engineering, October 21, 1949, p. 409.

BIBLIOGRAPHY

Vacuum Extraction Drying

Carpenter, A., "Drying of Hosiery Good," Textile Recorder, LXIX, No. 805, April 1950, pp. 84-85.

________, "High Efficiency Cylinder Drying Machine," Textile Recorder, LXXXI, No. 965, August 1963, pp. 68-70.

Goodings, A. C., "Air Flow Through Textile Fabrics," Textile Research Journal, XXXIV, No. 8, August 1964, pp. 713-724.

Jones, E. H., "Accelerated Cylinder Drying," Institute of Fuel Journal, XXX, No. 200, September 1957, pp. 506-510.

Mc Mahon, G. B. and J. G. Downes, "Propagation of Temperature and Moisture Changes During Forced Convective Flow of Air Through Mass of Hygroscopic Fibers, International Journal of Heat and Mass Transfer, V, July 1962, pp. 689- .

_______, "New Open Width Suction Extractor," Textile Recorder LXVII, No. 805, April 1950, pp. 84-85.

Perkins, F. M., H. McCall, H. F. Creegan and D. C. Glassford, "Drying Equipment and Dry of Textiles After Wet Processing," American Dyestuff Reporter, LI, No. 13, June 25, 1962, pp. 30-46.

Steel, R. "Factors Affecting Drying of Apparel Fabrics," Textile Research Journel, XXVIII, No. 2, February 1958, pp. 136-47.

Types of Separators

Kleinschmidt and Anthony, "Recent Development of Cyclone (Pease-Anthony) Scrubber," A.S.M.E. Transactions, LXIII, No. 349, 1941.

Perry, ed., "Cyclone Separators, "C. E. Engineers Handbook, 1950, p. 1023.

Peters, "Electrical Precipitators, "C. E. Engineers, 1963, pp. 20-80.

Cyclone Separators

Brookman, R. S., "Small Diameter Cyclones," Chemical Engineering Progress, LIX, No. 11, November 1963, pp. 66-69.

Caplan, K. J., "All About Cyclone Collectors," Air Engineering, VI, No. 9, September 1964, pp. 28-38.

Gallaer, C. A., "Mechanical Dust Collectors," Journal of Air Pollution Control Association, XIII, No. 12, 1963, p. 574.

Perry, ed., "Cyclone Separators," C. E. Engineers Handbook, 1950, p. 1023.

Pownall, J. H., "Cyclones in the Chemical and Process Industries," Chemistry and Industry, No. 47, November 25, 1961, p. 1888.

Stairmand,C. J. "Pressure Drop in Cyclone Separators," Engineering, October 21, 1949, p. 409.

ter Linden, A. J., "Investigations into Cyclone Dust Collectors," Institution of Mechanical Engineers, September 1949, p. 233.

APPENDIX

```
           ITERATION MAD COMPUTER PROGRAM

           DETERMINATION OF PRESSURE DROP IN A CYCLONE SEPARATOR FOR A
           CIRCULAR INLET DUCT AND NO REENTRAINMENT SHIELD

           INPUT DATA REQUIRED ARE
                Q-CFM, VOLUMETRIC FLOW RATE, NONSTANDARD
                P-PSI, AIR PRESSURE IN SEPARATOR
                T-DEGREES F, AVERAGE OF INLET AND OUTLET TEMPERATURES
                M-RATIO EXIT DUCT LENGTH INSIDE SEPARATOR/EXIT DUCT D
           N-RATIO OF SEPARATOR LENGTH/SEPARATOR DIAMETER

           TABLE OF REFERENCES
                DC- INCHES, SEPARATOR DIAMETER
                DI-INCHES, INLET DIAMETER
                DE-INCHES, EXIT DIAMETER
                LC-INCHES, LENGTH OF SEPARATOR
                LE-INCHES, LENGTH OF EXIT DUCT INSIDE SEPARATOR
                DELP-INCHES OF WATER, PRESSURE DROP ACROSS SEPARATOR
                VI- FEET/SEC., INLET VELOCITY
                K1=X- RATIO OF INLET DUCT DIAMETER/EXIT DUCT DIAMETER
                K2=Y-RATIO OF SEPARATER DIAMETER/EXIT DUCT DIAMETER
          REFERENCES ON
START     READ AND PRINT DATA Q,P,M,N,T
          THROUGH LOOP,FOR VI=100,5,VI.G.101
          DELP=5.E15
          THROUGH OVAL,FOR K1=.5,.1,K1.G.3
          THROUGH OVAL, FOR K2=1.5,.1, K2.G.3
          WHENEVER K1.E.K2, TRANSFER TO OVAL
          K3=(K2/K1).P.2*(N+.5+(M/K2.P.2))/50
          K4=1/(2*K2-2*K1)
          B=(K4+2*K3-     SQRT.(K4.P.2+4*K3*K4))/K3.P.2
          D=.00808*P*VI.P.2*(1+B*(1/K4-1)+2*K1.P.4)/(460+T)
          WHENEVER D.L.DELP
               DELP=D
               X=K1
               Y=K2
OVAL      END OF CONDITIONAL
          DI=1.75*SQRT.(Q/VI)
          DE=DI/X
          DC=DE*Y
          LC=N*DC
          LE=M*DE
LOOP      PRINT RESULTS DELP,VI,DC,DI,DE,LC,LE,X,Y
          TRANSFER TO START
          END OF PROGRAM


           Q=50,P=14.6,M=1.25,N=4,T=70*

               DELP =        4.872710,              VI =     100.000000
                 DC =        3.712311,              DI =       1.237437
                 DE =        2.474874,              LC =      14.849242
                 LE =        3.093592,               X =        .500000
                  Y =        1.500000
```

```
           COMPUTATION MAD COMPUTER PROGRAM

           DETERMINATION OF PRESSJRE DROP IN A CYCLONE SEPARATOR FOR A
           CIRCULAR INLET DUCT AND NO REENTRAINMENT SHIELD

           INPUT DATA REQUIRED ARE
                  Q-CFM, VOLUMETRIC FLOW RATE, NONSTANDARD
                  P-PSI, AIR PRESSJRE IN SEPARATOR
                  T-DEGREES F, AVERAGE OF INLET AND OUTLET TEMPERATURES
                  DC- INCHES, SEPARATOR DIAMETER
                  DE-INCHES, EXIT DIAMETER
                  DI-INCHES, INLET DIAMETER
                  LC-INCHES, LENGTH OF SEPARATOR
                  LE-INCHES, LENGTH OF EXIT DUCT INSIDE SEPARATOR

           TABLE OF REFERENCES
                  DELP-INCHES OF WATER, PRESSURE DROP ACROSS SEPARATOR
                  VI- FEET/SEC., INLET VELOCITY
           REFERENCES ON
START      READ AND PRINT DATA Q,P,T,DC,DI,DE,LC,LE
           K1=DI/DE
           K2=DC/DE
           N=LC/DC
           M=LE/DE
           VI=3.06*Q/(DI.P.2)
           K3=(K2/K1).P.2*(N+.5+(M/K2.P.2))/50
           K4=1/(2*K2-2*K1)
           B=(K4+2*K3-     SQRT.(K4.P.2+4*K3*K4))/K3.P.2
           D=.00808*P*VI.P.2*(1+B*(1/K4-1)+2*K1.P.4)/(460+T)
           DELP=D
           PRINT RESULTS DELP, Q,VI
           TRANSFER TO START
           END OF PROGRAM


Q=48.6,P=12.57,T=80,DC=6.5 ,DI=1.5,DE=2,LC=3.25,LE=2*

      DELP =      9.409287,               Q =      48.600000

        VI =     66.095999
```